CHAPTER SIX

Heterologous expression, purification, and characterization of proteins in the lanthanome

Emily R. Featherston, Joseph A. Mattocks, Jonathan L. Tirsch, and Joseph A. Cotruvo Jr.*

Department of Chemistry, The Pennsylvania State University, University Park, PA, United States *Corresponding author: e-mail address: juc96@psu.edu

Contents

1.	Introduction		120
2.	Purification and assay of native XoxF from M. extorquens AM1		122
	2.1 Notes on expression and	d purification	122
	2.2 Notes on dye-linked and	l XoxG-based activity assays	124
3.	XoxG		127
	3.1 Materials		128
	3.2 Expression and purificati	on of XoxG	129
	3.3 Determination of the ex	tinction coefficients of XoxG	131
	3.4 Determination of the red	duction potential of XoxG	132
4.	XoxJ		135
	4.1 Materials		136
	4.2 Expression and purificati	on of XoxJ	136
5.	Lanmodulin		139
	5.1 Materials		141
	5.2 Expression and purificati	on of LanM	141
	5.3 Determination of lantha	nide-binding stoichiometry using xylenol orange	144
6.	PqqT		147
	6.1 Materials		148
	6.2 Expression and purificati	on of PqqT	149
	6.3 Spectroscopic methods	to probe PQQ binding	150
7.	7. Summary		152
Ac	Acknowledgments		
Re	References		

Abstract

Recent work has revealed that certain lanthanides—in particular, the more earthabundant, lighter lanthanides—play essential roles in pyrroloquinoline quinone (PQQ) dependent alcohol dehydrogenases from methylotrophic and non-methylotrophic

bacteria. More recently, efforts of several laboratories have begun to identify the molecular players (the lanthanome) involved in selective uptake, recognition, and utilization of lanthanides within the cell. In this chapter, we present protocols for the heterologous expression in *Escherichia coli*, purification, and characterization of many of the currently known proteins that comprise the lanthanome of the model facultative methylotroph, *Methylorubrum extorquens* AM1. In addition to the methanol dehydrogenase XoxF, these proteins include the associated *c*-type cytochrome, XoxG, and solute binding protein, XoxJ. We also present new, streamlined protocols for purification of the highly selective lanthanide-binding protein, lanmodulin, and a solute binding protein for PQQ, PqqT. Finally, we discuss simple, spectroscopic methods for determining lanthanide- and PQQ-binding stoichiometry of proteins. We envision that these protocols will be useful to investigators identifying and characterizing novel members of the lanthanome in many organisms.

1. Introduction

Since the initial discovery in 2011 (Fitriyanto et al., 2011; Hibi et al., 2011), the lighter and most abundant members (La, Ce, Pr, Nd, Sm, and Eu) of the lanthanide (Ln) series—the 15 elements from La to Lu—have been shown to play essential catalytic and functional roles in biology, most notably in methylotrophic bacteria. Methylotrophic bacteria use reduced onecarbon compounds (e.g., methanol) as their sole carbon and energy source (Anthony, 1982; Chistoserdova, Kalyuzhnaya, & Lidstrom, 2009). The discovery that lanthanides are essential for catalysis in the most broadly distributed class of pyrroloquinoline quinone (PQQ)-dependent methanol dehydrogenases (MDHs), XoxF, has changed the field of methylotrophy as well as bioinorganic chemistry more generally. Although the XoxF-type lanthanide-dependent MDHs were discovered decades after their calciumdependent orthologs (Anthony & Williams, 2003), lanthanide-dependent methanol oxidation may be the ancestral process (Chistoserdova, 2011; Chistoserdova & Kalyuzhnaya, 2018; Keltjens, Pol, Reimann, & Op den Camp, 2014; Picone & Op den Camp, 2019). It is now clear that methylotrophic (and some non-methylotrophic) bacteria that utilize lanthanides occupy diverse habitats (Huang et al., 2019), from volcanic mudpots (Pol et al., 2014) to the phyllosphere (Ochsner et al., 2019) to freshwater and marine environments (Krause et al., 2017; Taubert et al., 2015).

The utilization of lanthanides by MDHs, other alcohol dehydrogenases (ADHs), and likely other enzymes, necessitates the involvement of many more proteins and other biomolecules in selective acquisition, trafficking, regulation, and utilization of these metal ions, which we have termed the

"lanthanome" (Cotruvo, 2019), the study of which is "lanthanomics." XoxF is encoded in an operon alongside genes encoding a c-type cytochrome, XoxG, the physiological electron acceptor for XoxF, as well as a periplasmic solute binding protein (SBP) of currently unknown function, XoxJ. Many lanthanide-dependent ADHs have been characterized, not limited to MDHs but also ethanol dehydrogenases, ExaF and PedH (Good et al., 2016; Wehrmann, Billard, Martin-Meriadec, Zegeye, & Klebensberger, 2017). Apart from these core ADH proteins, the first native lanthanide-binding protein to be discovered was lanmodulin (LanM), which uses metal-binding motifs similar to those of Ca^{II}-binding proteins to instead bind lanthanides with high affinity and high selectivity (Cook, Featherston, Showalter, & Cotruvo, 2019; Cotruvo, Featherston, Mattocks, Ho, & Laremore, 2018). This discovery led to identification of a gene cluster, of which lanM is a part, encoding several proteins involved in uptake and utilization of lanthanides in the model methylotroph, Methylorubrum extorquens (Mattocks, Ho, & Cotruvo, 2019; Ochsner et al., 2019), also later identified by transposon mutagenesis (Roszczenko-Jasińska et al., 2020). Together, these reports confirmed the involvement of metallophore-mediated lanthanide uptake suggested by early studies (Gu, Haque, Dispirito, & Semrau, 2016; Keltjens et al., 2014). Another protein in this cluster, LanD (META1p1781 or LutD) was also shown to directly bind lanthanides (Mattocks et al., 2019). In addition to genes involved in lanthanide metallophore (lanthanophore) uptake, this cluster may include other lanthanoenzymes and other lanthanide-binding proteins. In addition, one of the relatively small number of genes upregulated by lanthanides in M. extorquens has been characterized as a PQQ-binding SBP, putatively involved in PQQ uptake (Ho & Cotruvo, 2019). Identities of proteins potentially involved in PQQ transport from the cytosol (Roszczenko-Jasińska et al., 2020) and metal-PQQ chaperoning in the periplasm (Featherston & Cotruvo, 2021) have also been speculated. Important regulatory mechanisms have yet to be fully elucidated (Akberdin et al., 2018; Chu, Beck, & Lidstrom, 2016; Farhan Ul Haque et al., 2015; Gu & Semrau, 2017; Skovran, Raghuraman, & Martinez-Gomez, 2019; Wehrmann, Berthelot, Billard, & Klebensberger, 2018). Therefore, the lanthanome has expanded greatly in recent years and will surely continue to do so as more organisms and proteins involved in lanthanide biochemistry are characterized (Chistoserdova, 2019; Featherston & Cotruvo, 2021).

In this chapter, we present detailed methods for the heterologous expression, purification, and characterization of most of the presently confirmed

members of the lanthanome of M. extorquens AM1—XoxG, XoxJ, LanM, and PqqT—other than the alcohol dehydrogenases. Although strategies exist to purify these proteins from overexpression in M. extorquens AM1 (see chapters "Expression, purification and properties of the enzymes involved in lanthanide-dependent alcohol oxidation: XoxF4, XoxF5, ExaF/PedH, and XoxG4" by Huang et al. and "Expression, purification and testing of lanthanide-dependent enzymes in Methylorubrum extorquens AM1" by Good and Martinez-Gomez, in this volume), using Escherichia coli as the expression host may be preferable for some proteins: E. coli grow more quickly than M. extorquens, yields of proteins (once codon-optimized for expression in E. coli) are high, periplasmic extraction is easier in E. coli than in *M. extorquens*, and the required cells, vectors, and techniques are already in the possession of almost every biochemist. The high yields also facilitate the use of constructs without purification tags, which can affect protein function and are inefficient to remove using proteases. Finally, we also provide additional notes for each protein to provide context for its involvement in lanthanide biochemistry and to guide future studies in this new and rapidly changing field.



2. Purification and assay of native XoxF from *M. extorquens* AM1

Unlike the other proteins described in this chapter, in order to be active, XoxF must be purified from a suitable methylotrophic bacterium that can express the appropriate cofactor insertion machinery—at least until the nature of this machinery is better understood and can be replicated in another expression host. Here, we focus on important issues regarding expression, metalation, and assay of these enzymes.

2.1 Notes on expression and purification

Detailed protocols for growth of *M. extorquens* AM1 (ATCC 14718, NCIB 9133) in MP medium can be found in Delaney et al. (2013) and in chapters "Discovery of lanthanide-dependent methylotrophy and screening methods for lanthanide-dependent methylotrophs" by Tani et al., "Expression, purification and properties of the enzymes involved in lanthanide-dependent alcohol oxidation: XoxF4, XoxF5, ExaF/PedH, and XoxG4" by Huang et al., and "Expression, purification and testing of lanthanide-dependent enzymes in *Methylorubrum extorquens* AM1" by Good and Martinez-Gomez in the present volume. Protocols for purification of the native, untagged

protein from *M. extorquens* have been provided by Nakagawa and co-workers [(Nakagawa et al., 2012; Wang et al., 2020) and chapter "Discovery of lanthanide-dependent methylotrophy and screening methods for lanthanide-dependent methylotrophs" by Tani et al. in the present volume] and by our laboratory (Cotruvo et al., 2018; Featherston et al., 2019). [For XoxF from *M. fumariolicum*, we refer the reader to Pol et al. (2014).] These purification strategies are generally similar, including ammonium sulfate fractionation, cation exchange and hydrophobic interaction chromatography, and desalting.

Lanthanide-dependent ADHs are unusual among enzymes in that they can utilize multiple metal ions efficiently. The number of distinct lanthanides supporting catalysis in vitro and/or in vivo differs from enzyme to enzyme: e.g., La-Nd, La-Sm/Eu, or La-Gd, according to the XoxF clade in which an enzyme is found (Fitriyanto et al., 2011; Huang, Yu, & Chistoserdova, 2018; Lumpe, Pol, Op den Camp, & Daumann, 2018; Pol et al., 2014; Vu et al., 2016; Wehrmann et al., 2017). In the case of M. extorquens AM1, XoxF1 can be activated in vivo with La, Ce, Pr, and Nd, and poorly or not at all with Sm (Featherston et al., 2019; Good, Moore, Suriano, & Martinez-Gomez, 2019; Wang et al., 2020). The reasons for the inability to utilize later lanthanides are likely manifold—selectivity of the lanthanophore-mediated mechanism of uptake for early lanthanides (Mattocks et al., 2019), selectivity of trafficking and cofactor insertion machinery (Deblonde et al., 2020), stability of XoxF (Wang et al., 2020), and reduced efficiency of electron transfer to XoxG in Nd-XoxF vs. La-XoxF (Featherston et al., 2019). Related to XoxF purification, it is not necessarily true that production of XoxF for biochemical studies is equally effective with the four lightest lanthanides, La-Nd, when they are added individually to the growth media. Whereas researchers reporting metal contents of XoxF expressed in the presence of La, either from endogenous levels (Featherston et al., 2019; Nakagawa et al., 2012) or recombinantly in a methylotroph (Good et al., 2019; Huang et al., 2018), show roughly stoichiometric La incorporation, Nd incorporation is more variable. Purifying XoxF from endogenous levels, we observed similar protein yields and A_{280nm}/A_{359nm} ratio (Fig. 1, a measure of cofactor loading) for La, Ce, and Nd forms of XoxF, as well as similar activities (V_{max}) when measured using XoxG (Featherston et al., 2019). By contrast, plasmid-based expression of XoxF in the presence of Nd led to substoichiometric Nd insertion into XoxF (Good et al., 2019). Although the situation is clearly complex, one possible interpretation of these results is that plasmid-based XoxF overexpression in M. extorquens might cause Nd import to become limiting for

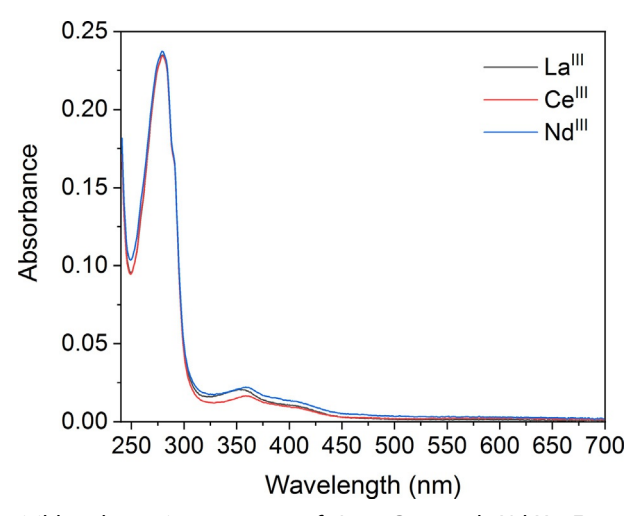
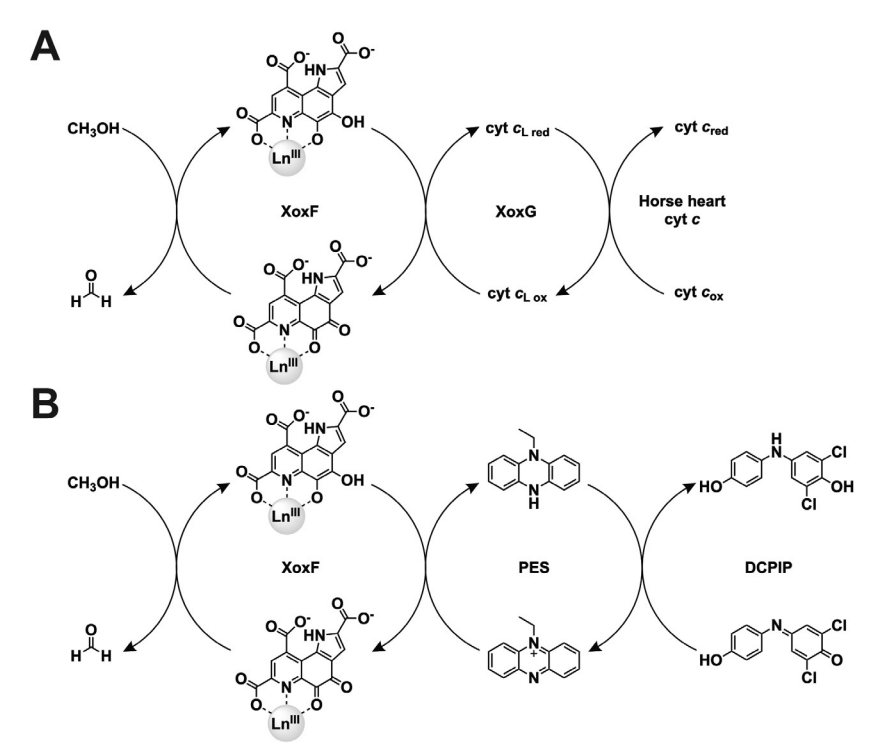


Fig. 1 UV–visible absorption spectra of La-, Ce-, and Nd-XoxFs purified from *M. extorquens*. PQQ-containing MDHs have characteristic absorption features around 350–360 nm with a shoulder at ~410 nm. The A_{280nm}/A_{359nm} ratio is similar for these three preparations. *Reproduced with permission from Featherston, E. R., Rose, H. R., McBride, M. J., Taylor, E. M., Boal, A. K., & Cotruvo, J. A., Jr. (2019). Biochemical and structural characterization of XoxG and XoxJ and their roles in lanthanide-dependent methanol dehydrogenase activity.* Chembiochem, 20, 2360–2372, copyright 2019 Wiley-VCH.

cofactor insertion, thereby reducing Nd incorporation into XoxF in a way not observed with La, if it is imported more efficiently. At endogenous levels of XoxF, less efficient Nd import may be less problematic. Further experiments with XoxFs metalated with different lanthanides will be important to address these questions.

2.2 Notes on dye-linked and XoxG-based activity assays

There are two types of activity assays for MDHs (Scheme 1): dye-linked and cytochrome-based, each of which can be carried out in cuvette or plate reader formats. For assay of chromatography fractions during purifications, activity can be determined by reduction of 2,6-dichlorophenolindolphenol (DCPIP) using phenazine ethosulfate (PES) as an electron acceptor, according to the method of Day and Anthony (Day & Anthony, 1990). Our minor modifications are reported in Cotruvo et al. (2018). Enzyme activity is reported in units (U), where 1U is defined as 1 µmol O₂ reduced per min between 15 and 30 s after initiating the reaction, which corresponds to 1 µmol DCPIP reduced/min. Because the extinction coefficient for DCPIP is pH dependent, we recommend that it be determined in assay



Scheme 1 XoxG-based (A) and dye-linked (B) assay systems for XoxF in M. extorquens. In vitro, horse heart cytochrome c is a convenient coupling protein because it is readily available. In vivo, another cytochrome (cytochrome c_H) is hypothesized to be the electron acceptor from XoxG. Reproduced with permission from Featherston, E. R., Rose, H. R., McBride, M. J., Taylor, E. M., Boal, A. K., & Cotruvo, J. A., Jr. (2019). Biochemical and structural characterization of XoxG and XoxJ and their roles in lanthanide-dependent methanol dehydrogenase activity. Chembiochem, 20, 2360–2372, copyright 2019 Wiley-VCH.

buffer by comparison with a stock solution prepared in 20 mM MOPS pH 7.0 [$\epsilon_{600\mathrm{nm}} = 20,600\,\mathrm{M}^{-1}\,\mathrm{cm}^{-1}$ at pH 7.0 (Armstrong, 1964)]. In the typical pH 9.0 assay buffer, we have determined $\epsilon_{600\mathrm{nm}} = 22,500\,\mathrm{M}^{-1}\,\mathrm{cm}^{-1}$. Activity assays on purified protein with the artificial, dye-linked system can be carried out on a plate reader by using a modification of these methods, described in detail in Featherston et al. (2019).

We note that chapter "Activity assays of methanol dehydrogenases" by Marie et al. in this volume also describes this method step by step, along with a protocol using an alternative mediator and chromophore that yields similar results. Any of these procedures can also be applied to assay the purified XoxF protein.

Activity assays of the purified protein can also be carried out using the physiological electron acceptor, XoxG (see Section 3 for purification and characterization procedures). Our protocol for XoxG-based assays is adapted from Day and Anthony (Day & Anthony, 1990), which was initially developed to assay the Ca-dependent MDH, MxaFI, with MxaG as electron acceptor, and is described in detail in Featherston et al. (2019). A similar protocol is described in chapter "Activity assays of methanol dehydrogenases" by Marie et al., this volume, based on the reports of Versantvoort et al. (2019) and Featherston et al. (2019).

There are certain points to keep in mind in comparing dye-linked vs. cytochrome-based assays. First, the two assays do not necessarily give the same value for enzyme specific activity. Anthony reported that assays of MxaFI with MxaG yielded lower activities than the dye-linked assay (Cox, Day, & Anthony, 1992; Day & Anthony, 1990), and we observed the same with La- and Ce-metalated XoxF (Featherston et al., 2019). This observation might indicate that interaction between MDH and its electron acceptor is rate-limiting for methanol oxidation in vivo. Second, multiple investigators, including ourselves, have reported lower activities ($V_{\rm max}$) by the dye-linked assay when Ln-MDHs of the XoxF5 clade (including the M. extorquens AM1 XoxF1 discussed here) are metalated with Nd vs. with La (Featherston et al., 2019; Good et al., 2019; Wang et al., 2020). This observation matches slower growth of the native organism in the presence of Nd vs. on La (Huang et al., 2018; Vu et al., 2016; Wang et al., 2020). By contrast, we showed that when La-, Ce-, and Nd-metalated XoxFs were assayed with XoxG as electron acceptor, the $V_{\rm max}$ values were not significantly different for the three enzymes, but the $K_{\rm m}$ for XoxG increased from 2.5 μ M for La-XoxF to 7.6 µM for Nd-XoxF. This result suggests that the slower growth of M. extorquens on Nd vs. on La may be due more so to impaired XoxF-XoxG electron transfer—due to impaired redox and/or structural matching of the two proteins (Featherston et al., 2019; Wang et al., 2020)—than on metal uptake and trafficking effects. These considerations emphasize the importance of assaying XoxFs with their native electron acceptors to extract information more relevant to physiological function than the dye-linked assay provides (Huang, Yu, & Chistoserdova, 2018). Although these early results have helped to formulate hypotheses about the effects of different lanthanides on Ln-ADH activity and lanthanidedependent growth, more studies are needed in a larger number of organisms to understand these phenomena more completely.



The physiological electron acceptor for XoxF is the c-type cytochrome, XoxG (also called a cytochrome c_L). A His-tagged XoxG was first purified by Chistoserdova and co-workers and shown to be able to be reduced by its associated XoxF (Zheng, Huang, Zhao, & Chistoserdova, 2018). We heterologously expressed and purified M. extorquens AM1 XoxG from E. coli, determined its kinetic parameters as electron acceptor for XoxF, determined its reduction potential, and solved its X-ray crystal structure (Featherston et al., 2019). This study revealed interesting differences relative to the cytochrome c_L associated with the Ca-dependent MDH, MxaG (O'Keeffe & Anthony, 1980; Williams et al., 2006), including an unusually low reduction potential (+172 mV vs. +256 mV), and different structure near the heme-binding pocket. Contemporaneously, the homologous protein from M. fumariolicum SolV, which is a fusion of XoxG and XoxJ and therefore called cytochrome c_{GI} , was reported and biochemically characterized (Versantvoort et al., 2019). Although its structure has not yet been reported, the reduction potential is more similar to that of MxaG (Kalimuthu, Daumann, Pol, Op den Camp, & Bernhardt, 2019); these differences in potential between the different Ln-MDH systems may reflect different metal tolerances of the organisms and their respective MDHs (Featherston et al., 2019). In addition to acting as electron acceptor during catalysis, XoxG may also play other yet to be defined roles in methylotrophy (Zheng et al., 2018).

E. coli is a facile expression system for c-type cytochromes like XoxG, but because these bacteria do not normally synthesize c-type cytochromes under aerobic conditions, cells must be co-transformed with a plasmid encoding the necessary cytochrome c maturation factors, pEC86 (Londer, 2011). As has been previously mentioned by other investigators, His-tags can sometimes interfere with heme loading to the protein (Londer, 2011). Therefore, our purification of XoxG utilized the untagged, wild-type protein. The purity and yield (\sim 6 mg per L culture) are more than sufficient for biochemical and crystallographic studies (Featherston et al., 2019), such that a purification tag is not necessary. The xoxG gene was codon-optimized (see Featherston et al. for the sequence) and cloned into pET-24a.

3.1 Materials

For expression and purification:

- Chemically competent or electrocompetent E. coli BL21 (DE3) cells
- Plasmids: pEC86 and pET-24a-XoxG
- Luria-Bertani (LB) media
- Terrific broth (TB) media
- Kanamycin
- Chloramphenicol
- Isopropyl β-D-1-thiogalactopyranoside (IPTG)
- 5 mM Magnesium sulfate (MgSO₄)
- 1 M Tris, pH 7.4
- DEAE Sepharose Fast Flow column
- Phenyl Sepharose 6 Fast Flow (low substitution) column
- Fast protein liquid chromatography (FPLC) instrument
- HiLoad Superdex 75 pg 16/600 column (120 mL)
- **Buffer G1:** 30 mM Tris, 20% (w/v) sucrose, 1 mM EDTA, pH 7.4
- **Buffer G2:** 50 mM Tris, pH 7.4
- **Buffer G3:** G2 with 35% sat. (194 g/L) ammonium sulfate
- **Buffer G4:** G2 with 20% sat. (106 g/L) ammonium sulfate
- **Buffer G5:** 20 mM MOPS, 100 mM KCl, pH 7.0
- **Buffer G6:** 20 mM MOPS, pH 7.0

For extinction coefficient determination:

- Quartz microcuvette
- Sodium dithionite
- Solution A (0.2M NaOH, 40% (v/v) pyridine, 500 μM potassium ferricyanide)
- Solution B (0.5 M sodium dithionite, 0.5 M NaOH)

For reduction potential determination:

- Quartz microcuvette with septum cap
- Appropriate redox dye (e.g., DCPIP, 2.5 mM)
- Sodium dithionite
- Xanthine (made fresh, 30 mM in 0.5 M NaOH)
- D-Glucose (1 M)
- Glucose oxidase (8 mg/mL in Buffer G5)
- Bovine liver catalase (made fresh, 1 mg/mL)
- Xanthine oxidase (25 μM in Buffer G5)

Note: The enzymes used for reduction potential determination are commercially available.

3.2 Expression and purification of XoxG

3.2.1 Protein expression

Co-transform E. ωli BL21 (DE3) cells with pET24a-XoxG and pEC86 (Cm^R) and plate on LB-agar plates containing kanamycin (Km; 50 µg/mL) and chloramphenicol (Cm; 30 µg/mL; antibiotic concentrations in all media), and grow at 30 °C.

Note: While the co-transformation can be done with chemically competent cells, efficiency is low, so electroporation of electrocompetent cells is recommended.

- 2. Use a single colony to inoculate a 2-mL Terrific broth (TB)-Km/Cm culture and grow overnight at 30 °C with 200 rpm shaking. Use this culture to inoculate a 100-mL culture at 100 × dilution, grown overnight under the same conditions.
- 3. Use the 100-mL culture to inoculate $2 \times 1.5 \, \text{L}$ TB-Km/Cm at $100 \times \text{dilution}$, and grow under the same conditions to $OD_{600 \text{nm}} \sim 0.6$ (8–9 h). At this point, induce protein expression by addition of isopropyl β -D-1-thiogalactopyranoside (IPTG) to a concentration of 1 μ M. After overnight growth (15 h), harvest cells by centrifugation (7 min, $7000 \times g$, 4°C). Pre-weigh the centrifuge bottle(s) before harvesting the culture. After centrifugation, pour off the LB supernatant and weigh to determine the mass of the cell pellet. Typical yield is $\sim 8 \, \text{g}$ cell paste per L culture.

Note: The IPTG concentration of $1 \,\mu\text{M}$ is not a typographical error. Using higher concentrations (even $2{\text -}10 \,\mu\text{M}$) yielded noticeably lower XoxG levels in the periplasmic extract (XoxG expression is immediately apparent from the red color of the heme). If this protocol is applied to other cytochromes c_{L} , we recommend an initial test experiment (200 mL growth) using different IPTG concentrations, then periplasmic extraction and comparison of extract color and bands by gel. This will allow rapid optimization of cofactor incorporation.

4. Immediately use the cell pellet to harvest the periplasmic fraction containing XoxG, according to the procedure below.

3.2.2 Protein purification

Maturation of c-type cytochromes occurs in the periplasm; therefore, rather than lysing whole cells, this protocol begins with isolation of the periplasmic fraction, using the osmotic shock method.

Tip: It is advised that you continue through at least to end of step 8 before pausing.

- 1. Pre-chill a solution of 5 mM MgSO₄ on ice.
- 2. Using a pipet-aid, resuspend the cell paste from above in 40 mL of Buffer G1 per gram of cell paste. After the cell paste is fully resuspended, stir at 150 rpm at room temperature for 10 min. This can be done directly in the centrifuge bottle.
- **3.** Centrifuge for $20 \,\text{min}$ at $8000 \times g$, $4 \,^{\circ}\text{C}$. Carefully decant the supernatant.
- 4. Resuspend the cell pellet in 20 mL/g (original wet weight) ice-cold 5 mM MgSO₄. Stir at 150 rpm for 10 min at 4 °C (in a cold room) and centrifuge for 10 min at 8000 × g, 4 °C. Carefully decant the red supernatant, which is the periplasmic extract, to a beaker and add a stir bar.
- **5.** While stirring the extract, add 0.05 volumes of 1 M Tris, pH 7.4 (e.g., 25 mL for 500 mL extract).

Note: Extraction efficiency can be visualized by SDS-PAGE. Note that full-length protein, not transported from the cytosol, will be present in the spheroplast, and the transported protein in the extract will be shorter due to signal peptide cleavage.

6. Equilibrate a DEAE Sepharose Fast Flow column (2.5 × 4 cm, 20 mL) in Buffer G2. Apply the periplasmic extract, collecting the flowthrough as a single fraction. Wash the column with 2 column volumes (CV) of Buffer G2, collecting as a single fraction. Combine the light-red flowthrough and wash fractions, which contain XoxG.

Note: This step removes DNA and some contaminating proteins, which is helpful for subsequent steps.

- 7. Prepare the combined flowthrough and wash fractions for hydrophobic interaction chromatography by adding solid ammonium sulfate slowly, with stirring, to 35% saturation (194 g/L at 4 °C) (Englard & Seifter, 1990). Meanwhile, equilibrate a Phenyl Sepharose 6 Fast Flow (low substitution) column (2.5 × 4 cm, 20 mL) in Buffer G3.
- Load the solution to the Phenyl Sepharose column; the column should turn pale red, indicating XoxG binding, and the flowthrough should be colorless.

Note: This is a convenient pause point for the night.

9. Wash the column with 5 CV of Buffer G3. Elute with 10 CV of Buffer G4 and collect fractions. XoxG-containing fractions can be pooled by inspection of their red color or, more quantitatively, by absorbance at

- 418 nm. Concentrate the protein to <2 mL using an Amicon Ultra 10-kDa MWCO centrifugal filter device.
- 10. Load protein solution onto a HiLoad Superdex 75 pg 16/600 FPLC column pre-equilibrated with Buffer G5, and elute at 0.75 mL/min with 1 CV of the same buffer, analyzing by A_{280nm} and A_{418nm}, and collecting 1.5 mL fractions. Pool fractions according to A_{418nm}; XoxG elutes at 67–77 mL. Freeze and store at -80 °C.

3.3 Determination of the extinction coefficients of XoxG

We have determined the absorption spectra and extinction coefficients of the oxidized and reduced forms of XoxG (Fig. 2) by the method of Barr and Guo (Barr & Guo, 2015), which is summarized here.

- 1. Prepare a $1 \, \text{mL}$, $\sim 20 \, \mu \text{M}$ solution of XoxG in Buffer G6 (for a novel homolog purified for the first time, use the extinction coefficients below in order to estimate the concentration).
- 2. Dilute half of this solution 2× in Buffer G6 and acquire a UV-visible absorption spectrum (240–800 nm). This will be the reference spectrum for oxidized XoxG.

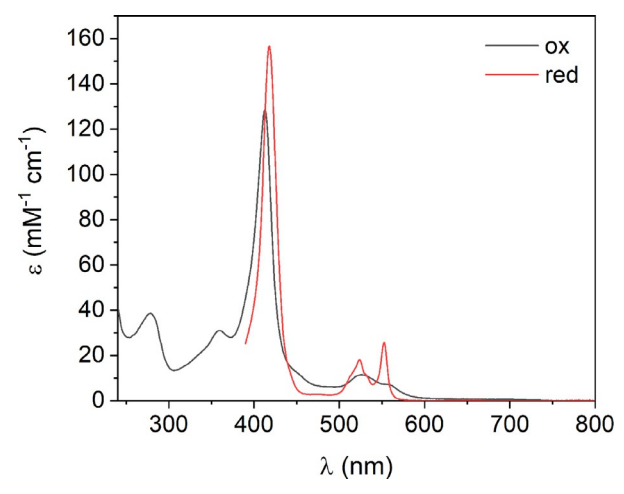


Fig. 2 UV–visible absorption spectra of oxidized (black) and dithionite-reduced (red) XoxG. *Reproduced with permission from Featherston, E. R., Rose, H. R., McBride, M. J., Taylor, E. M., Boal, A. K., & Cotruvo, J. A., Jr.* (2019). *Biochemical and structural characterization of XoxG and XoxJ and their roles in lanthanide-dependent methanol dehydrogenase activity.* Chembiochem, 20, 2360–2372, copyright 2019 Wiley-VCH.

3. Use a pipettor to dispense a few grains of sodium dithionite into the cuvette and mix, in order to fully reduce the protein, and acquire another spectrum. This will be the reference spectrum for reduced XoxG.

Note: Excess dithionite absorbs below \sim 400 nm, so the spectrum will be unreliable in that region.

- 4. Mix $250\,\mu\text{L}$ Buffer G6 and $250\,\mu\text{L}$ of Solution A (made fresh) and blank the spectrophotometer on this solution.
- 5. Mix $250\,\mu\text{L}$ of the $\sim\!20\,\mu\text{M}$ solution of XoxG from step 1 with $250\,\mu\text{L}$ of Solution A and take a spectrum.
- **6.** Add 5 μL of Solution B (made fresh) to the cuvette, mix quickly, and acquire a spectrum immediately and every minute until the spectrum no longer changes. Using the absorbance at 550 nm in the final spectrum, determine the concentration of heme [ε_{550nm}=30.27 mM⁻¹ cm⁻¹ for (pyridine)₂-heme ε].
- 7. Multiply this concentration by $505\,\mu\text{L}$ and divide by $250\,\mu\text{L}$. This will yield the concentration of heme in the $\sim\!20\,\mu\text{M}$ XoxG solution from step 1. Divide this value by 2 to determine the concentration of heme in the oxidized and reduced XoxG samples in steps 2 and 3. From these spectra and the heme concentration, calculate the extinction coefficients of XoxG.

Maximum absorptions for oxidized M. extorquens AM1 XoxG were determined as $\varepsilon_{413\mathrm{nm}} = 129\,\mathrm{mM}^{-1}~\mathrm{cm}^{-1}$ and $\varepsilon_{527\mathrm{nm}} = 11.5\,\mathrm{mM}^{-1}~\mathrm{cm}^{-1}$, and for the reduced form were $\varepsilon_{418\mathrm{nm}} = 157\,\mathrm{mM}^{-1}~\mathrm{cm}^{-1}$ and $\varepsilon_{553\mathrm{nm}} = 25.8\,\mathrm{mM}^{-1}~\mathrm{cm}^{-1}$. At the isosbestic point (413 nm), $\varepsilon = 129\,\mathrm{mM}^{-1}~\mathrm{cm}^{-1}$.

3.4 Determination of the reduction potential of XoxG

The reduction potential of the heme cofactor of XoxG can be determined spectrophotometrically, as described by Raven and co-workers (Efimov et al., 2014) based on a method developed by Massey (Massey, 1991). The method follows spectrophotometrically the reduction of a solution of the protein of interest and a redox-active organic dye standard. At a given time point, the concentrations of the oxidized and reduced forms of all redox-active species can be determined, from which the midpoint reduction potential ($E_{\rm m}$) of the protein can be calculated relative to the known potential of the dye. We found DCPIP, for which $E_{\rm m} = +217\,{\rm mV}$ at 25 °C, pH 7.0 (Clark, 1960), to be a useful dye for *M. extorquens* XoxG. Other dyes can be used instead, as long as the dye's $E_{\rm m}$ is within $\sim 50\,{\rm mV}$ of that of the protein. See Clark (1960) for a compilation of dyes and their reduction potentials.

- 1. Prepare the oxidized and reduced reference spectra for the dye. For DCPIP, determine the UV-visible spectrum of DCPIP_{ox} in the 350-800 nm range in Buffer G5 by using ε_{600nm} = 20.6 mm⁻¹ cm⁻¹, pH 7.0 (Armstrong, 1964), and determine the spectrum of DCPIP_{red} by addition of a slight excess of a freshly prepared solution of sodium dithionite. Convert the absorbance values at each wavelength to extinction coefficients.
- 2. In a total volume of 500 μL, mix the following in a septum-sealed, capped cuvette: Buffer G5, xanthine (300 μM), D-glucose (5 mM), glucose oxidase (25 μg), and bovine liver catalase (2.5 μg). Incubate the solution for 5 min with periodic inversion to achieve anaerobic conditions.

Note: D-glucose, glucose oxidase, and catalase act as an O_2 -scavenging system; glucose oxidase is a flavoprotein oxidase that reduces O_2 to H_2O_2 as part of its catalytic cycle, and catalase converts H_2O_2 to $1/2O_2$ and H_2O_3 .

3. Add XoxG (final concentration 4μM, from a stock of 250μM) and DCPIP (final concentration 25μM from a 2.5 mM stock) and mix. It is important to keep the volumes added small, to minimally affect anaerobiosis. Acquire an initial spectrum at 350–800 nm. Initiate reduction by addition of xanthine oxidase (20 nM), invert, and acquire spectra every minute for 40–60 min (4800 nm/min scan rate), until spectra are constant for >5 min (Fig. 3A).

Note: Depending on the activity of the xanthine oxidase preparation, the amount of enzyme may need to be adjusted. It is important that the rate of electron production by xanthine/xanthine oxidase not be too fast, to ensure that the system equilibrates throughout the titration. A total time of at least 40 min for the full reduction of the protein and dye is recommended.

- **4.** Using spreadsheet software, determine the initial concentrations of oxidized protein and oxidized dye by manual fitting of the initial spectrum in step 3 with spectra of DCPIP and XoxG.
- 5. For each time point, calculate the concentrations of DCPIP $_{\rm ox}$ and DCPIP $_{\rm red}$ from the $A_{600{\rm nm}}$ value (DCPIP $_{\rm red}$ and XoxG contribute negligibly to the $A_{600{\rm nm}}$ value and can be ignored); [DCPIP $_{\rm red}$] is equal to the difference between the initial [DCPIP $_{\rm ox}$] and [DCPIP $_{\rm ox}$] at each time point. These values reflect the solution potential at each time point.

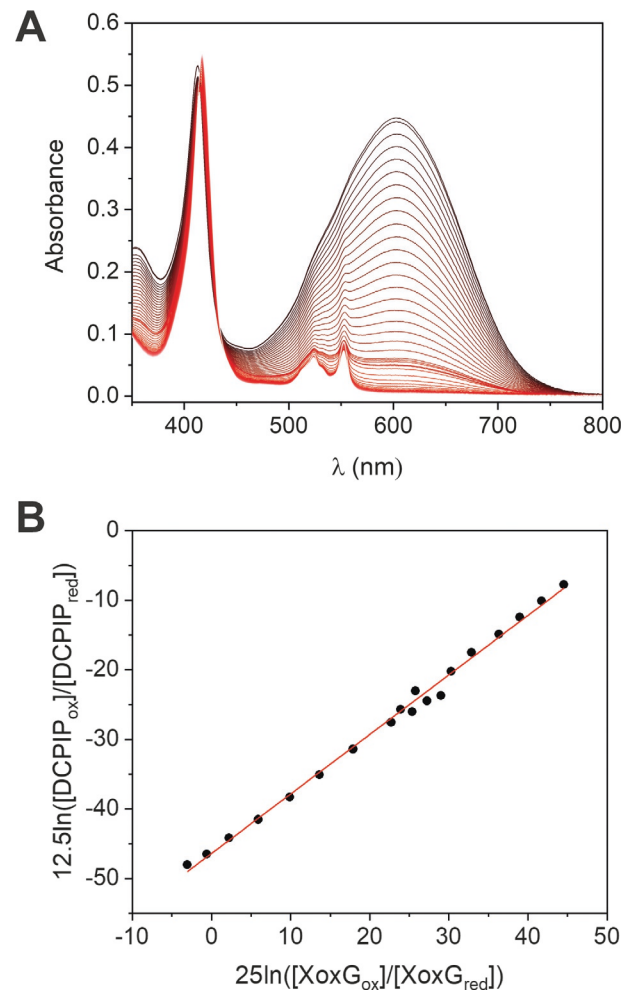


Fig. 3 Spectroscopic determination of XoxG reduction potential. (A) Spectroscopic titration of oxidized XoxG and DCPIP reduced by xanthine/xanthine oxidase over 1 h (black to red lines), with spectra acquired every 1 min. (B) Data analysis for the results in panel (A), according to steps 7 and 8. Reproduced with permission from Featherston, E. R., Rose, H. R., McBride, M. J., Taylor, E. M., Boal, A. K., & Cotruvo, J. A., Jr. (2019). Biochemical and structural characterization of XoxG and XoxJ and their roles in lanthanide-dependent methanol dehydrogenase activity. Chembiochem, 20, 2360–2372, copyright 2019 Wiley-VCH.

6. For each time point, calculate the concentration of reduced XoxG. First, subtract the contribution of DCPIP $_{\rm ox}$ (equivalent to [DCPIP $_{\rm ox}$] × $\epsilon_{418{\rm nm}({\rm DCPIP})}$) from $A_{418{\rm nm}}$. (Note that 418 nm is the $\lambda_{\rm max}$ for XoxG $_{\rm red}$.) Then, subtract the initial $A_{418{\rm nm}}$ contribution of XoxG $_{\rm ox}$. Finally, divide by the difference in extinction coefficient between the oxidized and reduced forms of XoxG at 418 nm, $\epsilon_{418{\rm red}} - \epsilon_{418{\rm ox}} = 56\,{\rm mM}^{-1}\,{\rm cm}^{-1}$.

This yields the concentration of $XoxG_{red}$. Subtract this value from the initial concentration of XoxG to yield the concentration of XoxG_{ox} at each time point. The concentrations of each of the redox species at each time point have now been calculated.

7. Determine the midpoint reduction potential (E_m) of XoxG. For each time point, determine (Eqs. 1 and 2):

$$y = 12.5 \ln \frac{[DCPIP_{ox}]}{[DCPIP_{red}]}$$

$$x = 25 \ln \frac{[XoxG_{ox}]}{[XoxG_{red}]}$$
(2)

$$x = 25 \ln \frac{[XoxG_{ox}]}{[XoxG_{red}]}$$
 (2)

8. Plot y vs. x and determine the regression line. The plot should have a slope of approximately 1, and the midpoint potential of the protein is determined from the y-intercept, which equals $E_{\rm m,protein} - E_{\rm m,dye}$, where $E_{\text{m,dve}}$ is the known reduction potential of the dye (Fig. 3B).

Note: The coefficients in Eq. (1) and (2) reflect the fact that the dye undergoes a two-electron reduction and XoxG undergoes one-electron reduction.

Note: Points at the beginning and end of the experiment may not be at equilibrium (apparent by deviation from linearity) and can be ignored in the analysis.

4. XoxJ

The third protein encoded by the core Ln-MDH operon is XoxJ. Like its analog in the Ca-MDH system, MxaJ, this protein is a member of the periplasmic (or solute) binding protein (PBP or SBP) family. SBPs are typically associated with recognition of ligands for membrane-bound transporters (Scheepers, Lycklama a Nijeholt, & Poolman, 2016), but XoxI and MxaJ are not obviously associated with such a system and their functions are unknown. However, the presence of a "J-type" SBP in the operons of PQQ-dependent alcohol dehydrogenases is conserved, and MxaJ (Amaratunga, Goodwin, O'connor, & Anthony, 1997; Van Spanning et al., 1991) and XoxJ (Roszczenko-Jasińska et al., 2020) are essential components of their respective MDH systems. The crystal structures of MxaJ (Choi, Cao, Kim, Lee, & Lee, 2017) and XoxJ (Featherston et al., 2019) reveal general architectures similar to classic SBPs, except they both exhibit exceptionally large cavities, putatively for substrate binding, as well as a β sheet missing several strands. Both of these features suggest that the substrate for XoxJ is likely a protein itself. We refer the reader to Featherston et al. (2019) for structural analysis of XoxJ and a more extended discussion of potential functions.

The protocol described here is expanded from the initial report by Featherston et al., with M. extorquens AM1 xoxJ having been codon-optimized and cloned into pET-24a. This procedure yields $\sim 3 \,\mathrm{mg}$ XoxJ per L culture.

4.1 Materials

- Reagents for cell growth and protein expression (see Section 3.1). All solid and liquid growth media contain 50 μg/mL kanamycin (Km)
- Ammonium sulfate
- 5 mM MgSO₄
- 1 M Tris, pH 7.4
- DEAE Sepharose Fast Flow column
- Phenyl Sepharose 6 Fast Flow (low substitution) column
- FPLC instrument
- HiPrep Phenyl FF (low sub) 16/10 column
- HiLoad 16/600 Superdex 200 pg column
- **Buffer J1:** 30 mM Tris, 20% (w/v) sucrose, 1 mM EDTA, pH 7.4
- **Buffer J2:** 50 mM Tris, 50 mM NaCl, pH 7.4
- Buffer J3: 50 mM Tris, 5% glycerol, pH 7.4, containing 35% sat. (NH₄)₂SO₄ (194 g/L)
- **Buffer J4:** 50 mM Tris, 5% glycerol, pH 7.4
- **Buffer J5:** 20 mM MOPS, 100 mM NaCl, pH 7.0

Buffers J1–J4 can be made by adding solids and/or glycerol to a minimal volume of water, adding the appropriate amount of the 1 M Tris stock solution given the final volume desired, and adding water up to volume. No pH adjustment is necessary.

4.2 Expression and purification of XoxJ

4.2.1 Protein expression

- Transform chemically competent E. coli BL21(DE3) cells with pET24a-XoxJ and grow at 37 °C overnight on LB-agar-Km plates. Use a single colony to inoculate 100 mL LB-Km and shake at 200 rpm overnight (~16h) at 37 °C.
- 2. Use this culture to inoculate three 2-L cultures of LB-Km (in 6L flasks) at 100 × dilution (20 mL each). Shake cultures at 200 rpm (37 °C) and monitor the OD_{600nm} periodically. At OD_{600nm} ~0.5, induce XoxJ

expression by adding IPTG to a concentration of $0.2 \,\mathrm{mM}$. After 2 h of induction, harvest cells by centrifugation (7 min, $7000 \times g$, 4°C). Preweigh the centrifuge bottle(s) before harvesting the culture. After centrifugation, pour off the LB supernatant and weigh to determine the mass of the cell pellet. Each liter of culture will yield $\sim 3 \,\mathrm{g}$ cell paste.

Note: Inducing at higher $OD_{600\mathrm{nm}}$ or for significantly more than 2h leads to insoluble material in the periplasmic extract without increasing protein yield. Therefore, inducing at $OD_{600\mathrm{nm}} = 0.5$ and for 2h is recommended.

3. Continue immediately with the periplasmic extraction procedure below.

Note: Do not freeze the cell pellet. Freezing it will cause cell lysis upon thawing.

4.2.2 Protein purification

This protocol uses the osmotic shock method for periplasmic extraction. Whereas periplasmic proteins like XoxJ can, in principle, be purified from the whole-cell lysate, we recommend extraction of the periplasm rather than whole-cell lysis for two reasons. First, relatively few proteins are present in the periplasm, so your protein of interest begins the purification procedure significantly purer than if cells were lysed. Second, the cytosolic fraction will likely contain your protein of interest that has not been exported, and therefore still contains its signal peptide, and may not have been folded or processed properly (e.g., in the case of XoxJ, formation of a disulfide bond).

Note: It is advised that you continue through at least to end of step 6 before pausing; pausing before running the periplasmic extract through the DEAE column leads to some precipitation overnight, which complicates subsequent steps.

- 1. Pre-chill a solution of 5 mM MgSO₄ on ice.
- 2. Using a pipet-aid, resuspend the cell paste from above in 40 mL of Buffer J1 per gram of cell paste. After the cell paste is fully resuspended, stir at 150 rpm at room temperature for 10 min. This can be done directly in the centrifuge bottle.
- **3.** Centrifuge for $20 \,\mathrm{min}$ at $8000 \times g$, $4 \,^{\circ}\mathrm{C}$. Carefully decant the supernatant.
- **4.** Resuspend the cell pellet in 20 mL/g (original wet weight) ice-cold 5 mM MgSO₄. Stir at 150 rpm for 10 min at 4 °C (in a cold room) and centrifuge for 10 min at 8000 × g, 4 °C. Carefully decant the supernatant, which is the periplasmic extract, to a beaker and add a stir bar.

 While slowly stirring the extract, add 0.05 volumes of 1 M Tris, pH 7.4 (e.g., 25 mL for 500 mL extract), and add solid NaCl to a final concentration of 50 mM.

Note: Extraction efficiency can be visualized by gel. Note that full-length protein, not transported from the cytosol, will be present in the spheroplast, and the transported protein in the extract will be shorter due to signal peptide cleavage.

Note: All of the subsequent chromatographic steps can be carried out either at room temperature or 4 °C.

6. Equilibrate a DEAE Sepharose Fast Flow column (2.5 × 4 cm, 20 mL) in Buffer J2. Apply the periplasmic extract, collecting the flowthrough as a single fraction. Wash the column with 5 CV of Buffer J2, collecting as a single fraction. Combine the flowthrough and wash fractions, which contain XoxJ.

Note: This step removes DNA and some contaminating proteins, which is helpful for subsequent steps.

Note: This is a convenient pause point for the night. Alternatively, you can pause after loading the gravity-flow Phenyl Sepharose column.

- 7. Prepare for hydrophobic interaction chromatography by adding solid ammonium sulfate slowly, with stirring, to 35% saturation (194g/L at 4°C) (Englard & Seifter, 1990). Equilibrate a Phenyl Sepharose 6 Fast Flow (low substitution) column (2.5 × 2 cm, 10 mL) in Buffer J3.
- 8. Load the solution to the Phenyl Sepharose column. Wash the column with 15 CV of Buffer J3. Elute with 10 CV Buffer J4 and collect in a single fraction. Concentrate the protein to <5 mL using an Amicon Ultra 10-kDa MWCO centrifugal filter device.

Note: The primary purpose of this step is to rapidly concentrate the protein so that it can be loaded more easily onto the FPLC. If you have a loop larger than 5 mL, the protein does not need to be concentrated as far.

- 9. Weigh out $(NH_4)_2SO_4$ (194 mg per mL of XoxJ, giving \sim 35% saturation) and dissolve in the concentrated XoxJ solution.
- 10. Purify XoxJ by FPLC using a hydrophobic column, e.g., HiPrep Phenyl FF (low sub) 16/10 column (GE Healthcare). Pre-equilibrate the column with Buffer J3, and load the protein using a 5 mL capillary loop. Wash the column at 2 mL/min with 4 CV Buffer J3, and elute with a 200 mL linear gradient of 0–100% Buffer J4 at 2 mL/min. Collect 4 mL fractions in peak fractionation mode (10 mAU threshold, detect A_{280nm} and A_{260nm}). XoxJ elutes as the major A_{280nm} peak,

- spanning 25–15% sat. $(NH_4)_2SO_4$. Pool these fractions and concentrate by centrifugal filtration (Amicon Ultra 10 kDa MWCO) to <2 mL.
- 11. In order to remove ammonium sulfate and a contaminating protein at ~15 kDa, purify XoxJ further by size-exclusion chromatography, e.g., on a HiLoad 16/600 Superdex 200 pg column. Pre-equilibrate the column with Buffer J5, and load the protein using a 2 mL capillary loop. Rinse the loop with 4 mL Buffer J5, and elute the column with 1 CV Buffer J5 at 0.75 mL/min. Collect 2 mL fractions.
- 12. Analyze fractions by SDS-PAGE, pool XoxJ-containing fractions, and concentrate by centrifugal filtration to the desired volume. XoxJ can be concentrated at least to $25 \, \text{mg/mL}$, which was the protein concentration used for crystallography (Featherston et al., 2019). Determine the protein concentration using $\varepsilon_{280 \, \text{nm}} = 34.0 \, \text{mM}^{-1} \, \text{cm}^{-1}$, estimated by ExPASy (Gasteiger et al., 2005).

Note: Purified XoxJ shows two bands on an SDS-PAGE gel. Mass spectrometry analysis suggests that the larger (minor) band corresponds to the protein after cleavage of the signal peptide before Gln27 (28.6 kDa), and the smaller (major) band corresponds to signal peptide cleavage before Leu32 (28.0 kDa) (Featherston et al., 2019). Because both bands are present throughout the purification, including in the whole-cell post-induction sample run on the gel, these results are consistent with alternative *E. coli* signal peptidase recognition sites, rather than proteolysis during purification. We have not been successful in separating these two forms, but the protein still crystallizes well, and the first residue visible in the structure is Val37.

5. Lanmodulin

Lanmodulin (LanM) was initially identified during a purification of XoxF from *M. extorquens* AM1, and it is the first natural, selective macrochelator for lanthanides to be discovered and characterized (Cotruvo et al., 2018). Its discovery also revealed the gene cluster responsible for uptake of lanthanides and delivery into the cytosol in this bacterium (Mattocks et al., 2019; Ochsner et al., 2019; Roszczenko-Jasińska et al., 2020). Although its function is not yet fully understood, it is one of a relatively small number of proteins upregulated in vitro and in planta in *M. extorquens* PA1 (along with XoxF, XoxG, XoxJ, PqqT, and three uncharacterized proteins) in response to lanthanum (Ochsner et al., 2019), and gene expression studies have also shown it to be upregulated in response to lanthanides in several other

bacteria (Masuda et al., 2018; Wegner, Gorniak, Riedel, Westermann, & Küsel, 2019). However, it is not essential for growth of *M. extorquens* in the presence of lanthanides, at least under the conditions studied to date (Ochsner et al., 2019; Roszczenko-Jasińska et al., 2020). In addition, although it is found in many alphaproteobacterial methylotrophs, it is not conserved in all lanthanide-utilizing bacteria (Chistoserdova, 2019; Cotruvo et al., 2018).

LanM consists of four 12-residue EF-hand motifs, each separated by 12-13 amino acid residues. EF-hand motifs are common recognition sites for Ca^{II} ions in biology (Gifford, Walsh, & Vogel, 2007), and, while these sites also non-specifically bind Ln^{III} ions (Drake, Lee, & Falke, 1996; Edington et al., 2018), LanM stands out for its tight and highly selective lanthanide binding. Biochemical studies revealed that the protein binds 3 equiv. of Ln^{III} ions with picomolar affinity (one in each of the first three EF hands), whereas the fourth EF hand does not bind metal ions tightly. LanM is largely disordered in its apo state, but in the presence of any rare earth, it adopts a compact, ordered form, stabilized by hydrophobic packing interactions as revealed by the NMR solution structure of the YIII-bound form (Cook et al., 2019). This conformational change is extremely (10⁸-fold) selective for lanthanides over Ca^{II} (Cotruvo et al., 2018) as well as for all non-rare earths tested to date (Deblonde et al., 2020). Although all lanthanides induce the conformational change at picomolar concentrations, the protein is biased toward the lighter Ln^{III} ions, albeit in an intriguing way: even though the biologically relevant early lanthanides bind more weakly to the protein than the later Ln^{III} ions (Deblonde et al., 2020), they more efficiently cause the conformational change of the protein (Cotruvo et al., 2018; Mattocks et al., 2019). For recent discussions of what this protein is teaching us about the principles of selective lanthanide recognition, and what is still yet to be learned, we refer the reader to Cotruvo (2019) and Featherston and Cotruvo (2021).

Initial expression studies in *E. coli* demonstrated that the protein was exported to the periplasm, and we verified the predicted signal peptide cleavage site. Yields of LanM purified from the periplasm were low. Because the protein contains no Cys residues (which could be oxidized to disulfides in the periplasm), we have found that higher protein yields are achievable via cytosolic expression of a construct with Ala22 as the first amino acid coded after the N-terminal Met. In our initial reports of LanM we used constructs that had a His₆-tag appended to either the N-terminus or C-terminus of the protein, which both yielded $\sim 20 \, \mathrm{mg/L}$ culture. Protocols for purification of those constructs can be found in Cotruvo et al. (2018).

However, we noticed that our yields were being limited by poor binding to the Ni-NTA column. Furthermore, and more importantly, we noted that the $\operatorname{Ln^{III}}$ -LanM K_d values for the C-terminally tagged protein were twofold higher than for the N-terminally tagged or untagged [produced by cleavage of the tag by tobacco etch virus (TEV) protease] proteins, an observation explained by the NMR structure (Cook et al., 2019). Therefore, we sought to develop a purification protocol for the wild-type protein, with no affinity tag.

Here, we introduce a purification protocol for wild-type LanM, with markedly improved yield (70–85 mg/L culture) relative to our initial reports. We also describe a simple method to determine metal-binding stoichiometry for lanthanide-binding proteins.

5.1 Materials

For purification:

- Reagents for cell growth and protein expression (see Section 3.1). All solid and liquid growth media contain 50 μg/mL kanamycin (Km)
- Protease inhibitor cocktail (e.g., Roche Complete Mini tablets)
- DNase I
- Phenylmethanesulfonyl fluoride (PMSF, 100 mM stock in isopropanol)
- Q-Sepharose Fast Flow
- FPLC instrument with S75 column (120 mL)
- **Buffer M1:** 50 mM Tris, 10 mM NaCl, 1 mM EDTA, 5% glycerol, pH 8.0
- Buffer M2: 50 mM Tris, 1 M NaCl, 1 mM EDTA, 5% glycerol, pH 8.0
- **Buffer M3:** 30 mM MOPS, 100 mM KCl, 5% glycerol, pH 7.0

For xylenol orange competition assay:

- **Buffer M4:** 20 mM MES, 20 mM acetate, 100 mM KCl, pH 6.1, stirred with 10 g/L Chelex-100 for 1 h followed by re-adjustment to pH 6.1
- Stock solution of 1.25 mM Ln^{III} of interest in Buffer M4
- Xylenol orange (XO), ~5 mM in water
- Quartz microcuvette

5.2 Expression and purification of LanM

5.2.1 Protein expression

1. Transform chemically competent *E. coli* BL21(DE3) cells with pET24a–LanM [this plasmid is analogous to those constructed to express the cytosolic LanM proteins initially described by Cotruvo et al., but without the His₆-tag] and grow at 37 °C overnight on LB-agar-Km plates. Use a

- single colony to inoculate 100 mL LB-Km and shake at 200 rpm overnight (~16h) at 37 °C.
- 2. Use this culture to inoculate one 2-L culture (in a 6-L flask) at 50 × dilution. Shake cultures at 200 rpm (37 °C) and monitor the OD_{600nm} periodically. At OD_{600nm} ~ 0.6, induce LanM expression by adding IPTG to a concentration of 0.2 mM.
- 3. After 3 h of induction, harvest cells by centrifugation (7 min, 7000 × g, 4 °C) and transfer to pre-weighed 50-mL conical tubes. Typical yield is ~2−3 g per L culture. Flash freeze cell paste in liquid nitrogen and store at −80 °C.

5.2.2 Protein purification

- 1. On ice, resuspend the cell pellet in 5 mL of Buffer M1 per g of cell paste. Buffer M1 should be supplemented with 1 protease tablet per 10 mL, DNase (2 U/mL), and PMSF (0.25 mM).
- 2. Lyse cells by sonication and pellet insoluble material by centrifugation at $40,000 \times g$, $45 \min$, 4° C.
- 3. The following step can be done at room temperature or in a cold room at 4 °C, as desired. Pre-equilibrate a 20 mL (2.5 × 4 cm) Q-Sepharose Fast Flow column in Buffer M1. Load the lysate to the column slowly, at ~2 mL/min. Wash column slowly with 1 CV Buffer M1.

Note: We find it easiest to run the Q-Sepharose step using a gravity-flow column, but the protocol can, of course, be adapted to an FPLC instrument.

4. Fill a gradient mixer (e.g., CBS Scientific GM-200) with 80 mL solutions of Buffer M1 and Buffer M2. Start the gradient and elute the protein from the Q-Sepharose column at the same flow rate as above. Collect 2 mL fractions in microcentrifuge tubes. It is only necessary to collect fractions for the first half (~80 mL) of the gradient, as LanM elutes with relatively high purity close to the beginning, at ~100−200 mM NaCl. Fractions can be screened by SDS-PAGE (16% Tris-Glycine). See Fig. 4A for a representative gel.

Note: LanM runs on the gel as a major band just above 10 kDa, in addition to several lower molecular weight bands [see fig. S7 in Cotruvo et al. (2018)]. Based on mass spectrometry analysis, these additional bands do not correspond to proteolysis; instead, they seem to be the result of multiple protein conformations, perhaps induced by adventitious trace metal binding.

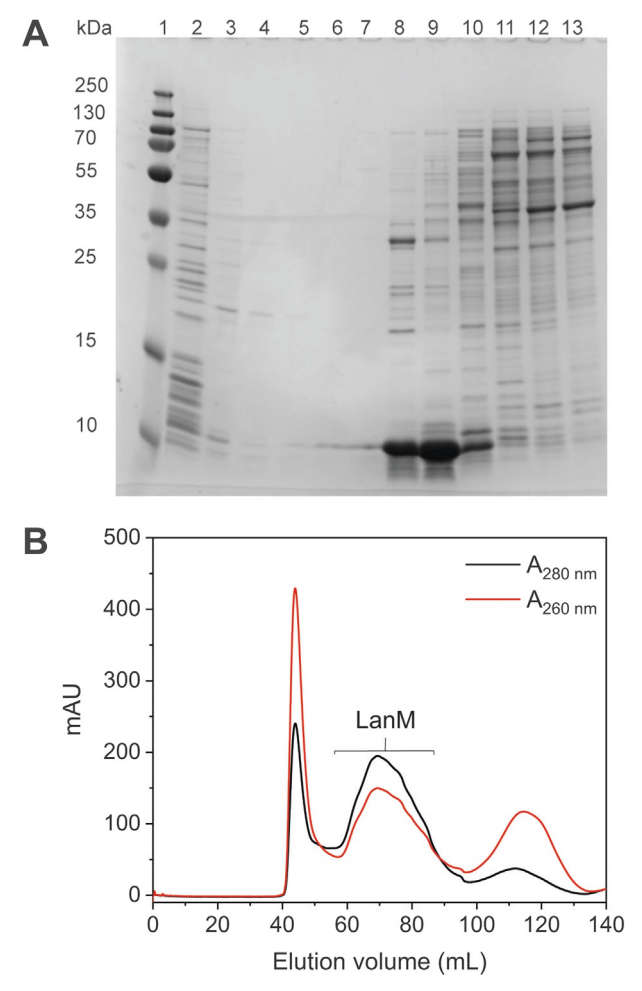


Fig. 4 Purification of wild-type LanM. (A) SDS-PAGE analysis of the Q-Sepharose column step, as follows: Lane 1, MW ladder; Lane 2, flowthrough; Lanes 3–5, wash fractions 1–3 (5–6 mL each); Lanes 6–13, elution fractions 1, 5, 10, 15, 20, 30, 35 (2 mL each). LanM is the strong band just above the 10 kDa marker, in lanes 8–10. (B) Chromatogram for the Superdex 75 pg step, displaying the broad elution of LanM. Fractions containing pure LanM are indicated.

- **5.** Pool desired fractions and concentrate by centrifugal filtration (Amicon Ultra 10kDa MWCO) to <2 mL.
- **6.** In order to remove DNA and minor contaminating proteins, load protein solution onto a HiLoad Superdex 75 pg 16/600 column pre-equilibrated with Buffer M3 and load the protein using a 2 mL capillary loop.

Rinse the loop with 2 mL Buffer M3 and elute with 1 CV of the same buffer at 0.75 mL/min. Follow elution at 280 and 260 nm. Collect 2 mL fractions.

Note: The elution profile will be a broad peak between \sim 60 and 85 mL on the 120 mL Superdex 75 pg column (Fig. 4B). This result is presumably associated with intrinsic disorder of the apoprotein as well as, perhaps, weak binding of trace metals in the buffer.

- 7. Pool LanM-containing fractions based on SDS-PAGE analysis and concentrate to the desired volume (e.g., 2 mL) by centrifugal filtration (10 kDa MWCO). Add 5 g Chelex-100 to 500 mL Buffer M3 and stir in a beaker at room temperature. Add LanM to a dialysis cassette (e.g., Slide-A-Lyzer MWCO 3500) or dialysis tubing and dialyze overnight at room temperature.
- 8. Determine the protein concentration using ε_{275nm}=1400 M⁻¹ cm⁻¹ (Cotruvo et al., 2018). *M. extorquens* LanM possesses one tyrosine, no tryptophans, and three phenylalanines; the fine structure below 275 nm associated with Phe absorption should be visible if the protein preparation has high purity [fig. S8 in Cotruvo et al. (2018)]. Freeze protein in liquid nitrogen at ~1 mM.

5.3 Determination of lanthanide-binding stoichiometry using xylenol orange

A fast and simple method to determine the lanthanide-binding stoichiometry of a newly isolated protein is an assay using xylenol orange (XO) as a competitive colorimetric reagent. A solution (pH 6.1) contains the protein of interest and XO, into which a solution of a lanthanide ion of interest is titrated. The affinity of XO for Ln^{III} ions under these conditions is in the $1-10\,\mu\text{M}$ range (Munshi & Dey, 1968; Tonosaki & Otomo, 1962); therefore, if the protein has high-nanomolar affinity for Ln^{III} ions, or better, it will preferentially bind the metal ions, and the spectrum of XO will remain unchanged. Once the protein's metal-binding site(s) is (are) saturated, the metal will instead bind to the dye, leading to an increase in the absorbance at \sim 575 nm. From the volume of titrant added to reach the first increase of XO absorption, the metal-binding stoichiometry of the protein can be calculated. This method is a useful preliminary experiment before more timeand protein-intensive methods to determine binding affinities are pursued, such as isothermal titration calorimetry (Quinn, Carpenter, Croteau, &

Wilcox, 2016) or the spectrophotometric methods described in chapters "Spectrophotometric methods to probe the solution chemistry of lanthanide complexes with macromolecules" by Deblonde and "Determination of affinities of lanthanide-binding proteins using chelator-buffered titrations" by Mattocks et al. of the accompanying volume, Volume 651.

For best results, we suggest ${\sim}10{-}20\,\mu\text{M}$ metal-binding sites in solution. In the method below, we use $5\,\mu\text{M}$ LanM, because it binds 3 equiv. of Ln^III ions tightly—the average stoichiometry across all of the lanthanides determined using this method is 2.9 ± 0.3 [see fig. S11 in Cotruvo et al. (2018]. When we applied this method to demonstrate that LanD (META1p1781 or LutD) binds 1 equiv. of Ln^III ions, we used $10\,\mu\text{M}$ (Mattocks et al., 2019). In the latter case, interestingly, the relative K_ds of XO and LanD were such that the protein outcompeted XO for light Ln^III ions (La-Gd) but not heavy Ln^III ions (roughly Ho-Lu) [see fig. S17 in Mattocks et al. (2019)].

We note that there is a relatively narrow range of pH in which xylenol orange is an effective colorimetric reagent for Ln^{III} ions (Lyle & Rahman, 1963); therefore, control of the pH is important during the experiment.

- 1. Blank the UV–visible spectrophotometer (240–800 nm) with a microcuvette containing $500\,\mu\text{L}$ of Buffer M4.
- 2. Add your protein of interest to the microcuvette to a concentration of $\sim 5\,\mu\text{M}$, and collect a spectrum over the 240–800 nm region. Calculate the protein concentration using a known extinction coefficient.

Note: An accurate starting protein concentration is important for quantitative analysis of metal-binding stoichiometry.

Note: Because of the pH sensitivity of the assay, if the protein is stored in a buffer at a different pH, it should either be quite concentrated (e.g., for LanM, ~1 mM) or the protein should be exchanged into Buffer M4 before dilution for the assay.

- 3. Add XO to a final concentration of \sim 5 μ M and collect a spectrum in the 240–800 nm region.
- 4. Titrate $1.25 \, \text{mM} \, \text{LnCl}_3$ solution in $0.5 \, \mu \text{L}$ aliquots (0.25 equiv. if $5 \, \mu \text{M}$ protein is present), mix, and acquire spectra between 240 and 800 nm after each addition.

Note: To mix, either use a P200 pipettor or invert the cuvette with parafilm on top. If you do the latter, use a different spot on the parafilm each time mixing in order to avoid a color change before the actual endpoint of the titration.

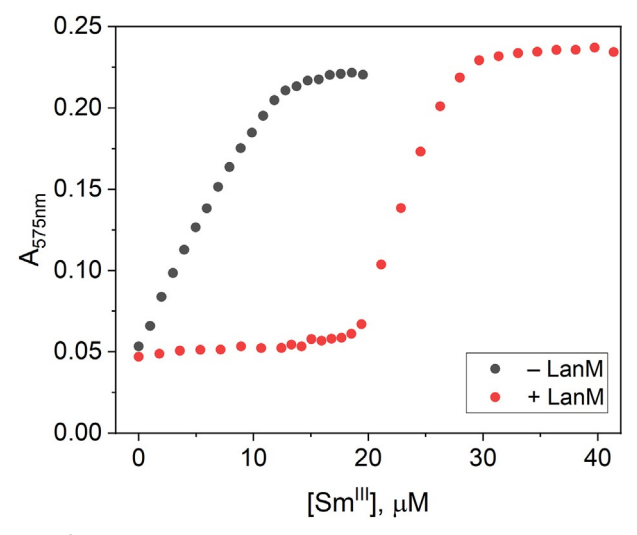


Fig. 5 Titration of xylenol orange with SmCl₃ in the presence and absence of LanM, monitored at 575 nm. The concentration of LanM in the experiment was 6.0 μM. The endpoint calculated by the method described in the text was at 19.4 μM Sm^{III}, which corresponds to 3.2 equiv. Adapted with permission from Cotruvo, J. A., Jr., Featherston, E. R., Mattocks, J. A., Ho, J. V., & Laremore, T. N. (2018). Lanmodulin: A highly selective lanthanide-binding protein from a lanthanide-utilizing bacterium. Journal of the American Chemical Society, 140, 15056–15061. Copyright 2018 American Chemical Society.

5. Continue the titration until there is no further change in the Ln^{III} -XO absorption feature at \sim 575 nm (λ_{max} is dependent on Ln^{III} ion in the experiment).

Note: Commercially available XO is impure, as evidenced by lack of precise isosbestic points during titrations. This fact does not affect the result of the titrations.

6. Correct the raw spectra for baseline drift and for volume change of the solution upon each addition of metal stock. Plot the corrected absorption at the $\lambda_{\rm max}$ of ~ 575 nm for each titration point against the metal ion concentration (Fig. 5). The metal ion concentration at which $A = A_{\rm initial} + 0.1$ ($A_{\rm final} - A_{\rm initial}$), the point of 10% saturation of XO, is taken as an estimate of the point at which the tight binding ($\ll \mu M$) sites of the protein of interest are saturated.

Note: XO adheres slightly to the microcuvette; after each experiment, we suggest filling the cuvette with 6M HCl and letting it sit for 5–10min, followed by your typical cuvette washing procedure (e.g., rinsing with water and acetone).



Decades of work, especially by Klinman and co-workers, has recently resulted in elucidation of the mechanism of biosynthesis of the organic cofactor of the ADHs, pyrroloquinoline quinone (PQQ) (Duine, 1999; Koehn et al., 2019; Zhu & Klinman, 2020), which occurs in the cytosol. However, less is known about PQQ trafficking once synthesized. The enzymes that use the cofactor are periplasmic, and it is also known that the cofactor is released into growth media by some of the bacteria that synthesize it (van Kleef & Duine, 1989). Furthermore, not all organisms that encode PQQ-dependent enzymes are able to make the cofactor, suggesting that PQQ transfer between organisms is important in the biosphere, as is the case for other cofactors such as cobalamins (Shelton et al., 2019).

Interested in investigating this exchange of PQQ between organisms, we hypothesized that a mechanism for PQQ uptake might exist. M. extorquens AM1 META1p1737 was a putative SBP encoded, along with putative ABC transporter subunits, by genes adjacent to xoxF. Like LanM, this protein is one of the handful of proteins upregulated by the presence of lanthanides in the growth medium of M. extorquens (Good et al., 2019; Ochsner et al., 2019). Using spectrophotometry, spectrofluorometry, and isothermal titration calorimetry (ITC), we demonstrated that this SBP, which we named PqqT, binds PQQ tightly (Ho & Cotruvo, 2019). We note that PQQ transport activity of the full system (a putative "PqqTUV" system) has not yet been demonstrated in cells, and the structure of protein has not yet been reported. We proposed that the function of cytosolic PQQ uptake might be to supplement the pool of the cofactor endogenously biosynthesized. It may also suggest that, even though the cofactor is used in the periplasm, that exogenous PQQ cannot equilibrate with the periplasmic pool used for ADH activation, for reasons of regulation and/or proper cofactor chaperoning.

As is its mechanism of biosynthesis, the solution chemistry and spectroscopy of PQQ are complex. In aqueous solution, PQQ exists in an equilibrium between its hydrated and unhydrated forms (Scheme 2). This equilibrium is also altered by the presence of nucleophiles and metal ions (Dekker, Duine, Frank, Verweil, & Westerling, 1982; Lumpe & Daumann, 2019). However, because these forms have different absorption and fluorescence properties, they can be used in certain cases to study PQQ binding to proteins, as has been done with the PQQ biosynthetic protein PqqC (Magnusson, RoseFigura,

Scheme 2 Hydration equilibrium speciation for PQQ. Reproduced with permission from Ho, J. V., & Cotruvo, J. A., Jr. (2019). A periplasmic binding protein for pyrroloquinoline quinone. Biochemistry, 58, 2665–2669. Copyright 2019 American Chemical Society.

Toyama, Schwarzenbacher, & Klinman, 2007) and with PqqT (Ho & Cotruvo, 2019). The affinities of these proteins for PQQ are 2 nM for the former and 50 nM for the latter.

Here we describe a new purification method for PqqT as well as provide helpful information for investigation of PQQ binding. As discussed in our original report, native PqqT possesses a Cys residue (C192) that is desulfurated to Ala when exported to the periplasm in *E. coli*, a modification that does not affect PQQ binding. Therefore, we will use a C192A variant, cloned into pET24a, that can be expressed in the cytosol (with Ala28 as the first residue), which yields 5 mg PqqT per L culture. A form with the Cys can be studied, but it requires an anaerobic spectroscopy setup (see our paper for a description). Further work is necessary to determine whether the Cys, while dispensable for PQQ binding in vitro, is playing a functional role in vivo. By discussing the case of PqqT here, we aim to provide guidance for researchers who wish to use these methods to investigate PQQ-binding proteins. Of course, PQQ will not necessarily undergo these same changes upon protein binding in all cases, as these changes depend on affinity and the structure of the binding site.

6.1 Materials

- Reagents for cell growth and protein expression (see Section 3.1). All solid and liquid growth media contain 50 μg/mL kanamycin (Km)
- Protease inhibitor cocktail (e.g., Roche Complete Mini tablets)
- DNase I
- Phenylmethanesulfonyl fluoride (PMSF, 100 mM stock in isopropanol)
- Q-Sepharose Fast Flow
- FPLC instrument

- HiLoad Superdex 75 pg 16/600
- Buffer T1: 50 mM Tris, 10 mM NaCl, 1 mM EDTA, pH 8.0
- **Buffer T2:** 50 mM Tris, 300 mM NaCl, 1 mM EDTA, pH 8.0
- **Buffer T3:** 30 mM MOPS, 100 mM KCl, pH 7.0

6.2 Expression and purification of PqqT

6.2.1 Protein expression

- 1. Transform chemically competent *E. woli* BL21(DE3) cells with pET24a–PqqT(C192A) and grow at 37 °C overnight on LB-agar-Km plates. Use a single colony to inoculate 100 mL LB-Km and shake at 200 rpm overnight (~16 h) at 37 °C.
- 2. Use this culture to inoculate one 2-L culture (in a 6-L flask) at $50 \times$ dilution. Shake cultures at $200 \, \text{rpm}$ (37 °C) and monitor the $OD_{600 \, \text{nm}}$ periodically. At $OD_{600 \, \text{nm}} \sim 0.6$, cool the flasks in a 4 °C cold room for 15 min and lower the temperature of the shaker to 18 °C. Return flask to the shaker and induce PqqT expression by adding IPTG to a concentration of $0.2 \, \text{mM}$.
- 3. After induction overnight (~18 h), harvest cells by centrifugation (7 min, 7000 × g, 4 °C) and transfer to pre-weighed 50-mL conical tubes. Typical yield is ~2.5 g per L culture. Flash freeze cell paste in liquid nitrogen and store at −80 °C.

6.2.2 Protein purification

- 1. On ice, resuspend the cell pellet in 5 mL of Buffer T1 per g of cell paste. Buffer T1 should be supplemented with 1 protease tablet per 10 mL, DNase (2 U/mL), and PMSF (0.25 mM).
- **2.** Lyse cells by sonication and pellet insoluble material by centrifugation at $40,000 \times g$, 20 min, $4 ^{\circ}\text{C}$.
- **3.** Pre-equilibrate a $15\,\text{mL}$ ($2.5\times3\,\text{cm}$) Q-Sepharose Fast Flow column (gravity-flow) in Buffer T1. Load the lysate to the column slowly. Wash column with 2 CV Buffer T1.
- **4.** Fill a gradient mixer (e.g., CBS Scientific GM-200) with 70 mL solutions of Buffer T1 and Buffer T2. Start the gradient and elute the protein from the Q-Sepharose column. Collect 1 mL fractions in microcentrifuge tubes and screen by SDS-PAGE. PqqT (32 kDa) elutes at ~100–200 mM NaCl.
- **5.** Pool desired fractions and concentrate by centrifugal filtration (Amicon Ultra 10kDa MWCO) to <2 mL.

- 6. Load protein solution onto a HiLoad Superdex 75 pg 16/600 column pre-equilibrated with Buffer T3 and load the protein using a 2 mL capillary loop. Rinse the loop with 2 mL Buffer M3 and elute with 1 CV of the same buffer at 0.75 mL/min. Follow elution at 280 and 260 nm. Collect 1.5 mL fractions. PqqT elutes at ∼60−70 mL.
- 7. Pool fractions based on SDS-PAGE analysis and concentrate to the desired volume by centrifugal filtration (10 kDa MWCO). Determine the protein concentration using $\varepsilon_{280\text{nm}} = 32.4 \text{mM}^{-1} \text{ cm}^{-1}$, estimated using ExPASy (Gasteiger et al., 2005), and store at $-80 \,^{\circ}\text{C}$.

6.3 Spectroscopic methods to probe PQQ binding

As noted above, binding of PQQ to proteins may be amenable to several spectroscopic approaches, taking advantage of spectral shifts in the PQQ/hydrate equilibrium (Scheme 2) and possibly other interactions accompanying protein binding. If observed, these shifts can be used to determine stoichiometry and even affinity. Titrations may be carried out in either direction; because it is the change in the PQQ spectrum associated with protein binding that is being monitored in these experiments, however, it is easier to start with PQQ in the cuvette and titrate protein into it.

For absorbance measurements, PQQ concentration is determined spectrophotometrically using $\varepsilon_{322\mathrm{nm}} = 8963\,\mathrm{M}^{-1}\,\mathrm{cm}^{-1}$, which is an isosbestic point between the two forms (Dekker et al., 1982). In our experiments, we focused on binding stoichiometry, so the PQQ and PqqT concentrations were >100-fold higher than the K_{d} to ensure full binding. Fig. 6A shows that the UV–visible spectrum of PQQ is increasingly perturbed as PqqT is titrated in; at the endpoint of the titration, the spectrum resembles that of the unhydrated cofactor—suggesting that the protein specifically recognizes it over the PQQ-hydrate.

The fluorescence spectrum of PQQ in aqueous solution ($\lambda_{\rm ex} = 375\,{\rm nm}$) exhibits a broad emission centered at 488 nm. This spectrum was suggested by early studies to be attributable largely to the PQQ-hydrate, with PQQ itself having little or no fluorescence (Dekker et al., 1982). Prior titrations of PQQ with PqqC showed a bathochromic shift of this emission to $\lambda_{\rm max} = 442\,{\rm nm}$, accompanied by an enhancement of the fluorescence, upon binding of PQQ to the enzyme (Magnusson et al., 2007). In the case of PqqT, the fluorescence emission also exhibits a bathochromic shift in the presence of the protein, but only to 470 nm, and the intensity of the resulting signal decreases significantly compared to that of the cofactor in solution

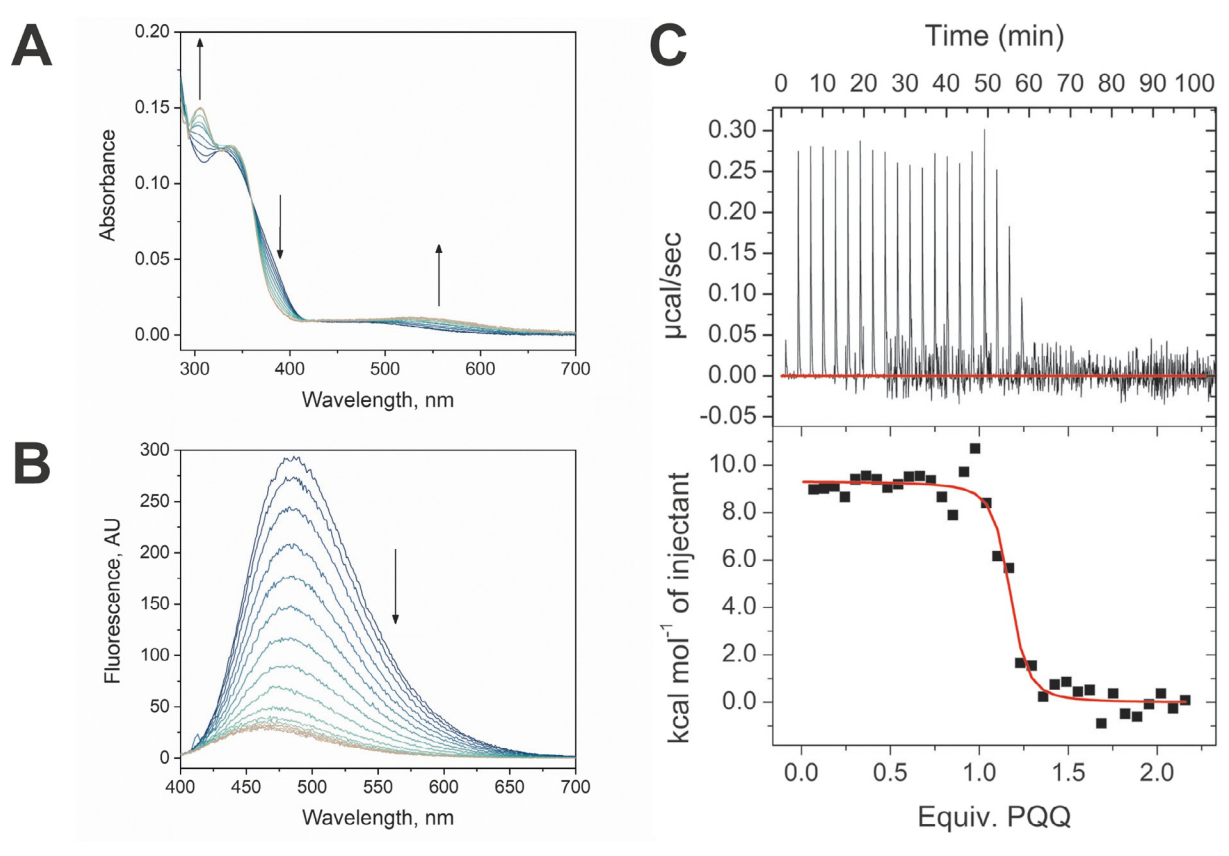


Fig. 6 Biophysical methods to study PQQ binding to PqqT. (A) Spectrophotometric titration of 13 μM PQQ with 0–18 μM PqqT in 1.5 μM increments (dark blue to gray). Binding stoichiometry (1.1 PQQ/PqqT) can be estimated once PqqT addition no longer alters the spectrum of PQQ. (B) Spectrofluorometric titration of 13 μM PQQ with 0–20 μM PqqT in 1 μM increments (dark blue to gray). Binding stoichiometry (1.3 PQQ/PqqT) can be estimated once PqqT addition no longer alters the spectrum of PQQ. (C) ITC analysis of PQQ binding to PqqT, yielding a K_d = 50 nM and n = 1.2. Adapted with permission from Ho, J. V., & Cotruvo, J. A., Jr. (2019). A periplasmic binding protein for pyrroloquinoline quinone. Biochemistry, 58, 2665–2669. Copyright 2019 American Chemical Society.

(Fig. 6B) (Ho & Cotruvo, 2019). We suggested that this might represent the fluorescence spectrum of the unhydrated PQQ (which to the best of our knowledge has not been definitively reported); however, the spectral shifts of PQQ accompanying binding to PqqT are not identical to those with PqqC. Structural characterization of the PqqT-PQQ complex will help to resolve this point.

Spectrofluorometric titrations can also be used to determine the protein-PQQ K_d if the concentration of PQQ in the experiment is on a similar order to the K_d . We refer the reader to Magnusson et al. (2007) for the application of this approach to PqqC. Binding affinity can also be determined by ITC, which also provides other thermodynamic parameters such as stoichiometry, enthalpy, and entropy change (Fig. 6C). For a practical summary of the ITC technique, see Pierce, Raman, and Nall (1999); for a more involved discussion of the theory, see Indyk and Fisher (1998). A protocol for ITC study of PqqT is provided in Ho and Cotruvo (2019).

7. Summary

We have provided detailed protocols for expression, purification, and characterization of proteins involved in lanthanide and PQQ utilization in *M. extorquens* AM1. These proteins, the first representatives of the lanthanome to be characterized beyond the ADHs, illustrate the ability to use the facile and ubiquitous *E. coli* expression platform to yield wild-type proteins (without affinity tags) from either the cytosol or periplasm. With defined protein expression and purification methods available and assay protocols developed, these methods can be easily applied to proteins from other lanthanide-utilizing organisms to expand our knowledge of the biochemistry of lanthanide and PQQ acquisition, trafficking, and utilization.

Acknowledgments

This work was supported by the National Science Foundation (CHE-1945015 to J.A.C.). J.A.C. also acknowledges the Pennsylvania State University Department of Chemistry and a Louis Martarano Career Development Professorship for support.

References

Akberdin, I. R., Collins, D. A., Hamilton, R., Oshchepkov, D. Y., Shukla, A. K., Nicora, C. D., et al. (2018). Rare earth elements alter redox balance in Methylomicrobium alcaliphilum 20Z(R). Frontiers in Microbiology, 9, 2735. https://doi.org/10.3389/finicb.2018.02735.

- Amaratunga, K., Goodwin, P. M., O'connor, C. D., & Anthony, C. (1997). The methanol oxidation genes mxaFJGIR(S)ACKLD in Methylobacterium extorquens. FEMS Microbiology Letters, 146, 31–38. https://doi.org/10.1111/j.1574-6968.1997.tb10367.x.
- Anthony, C. (1982). The biochemistry of methylotrophs. London: Academic.
- Anthony, C., & Williams, P. (2003). The structure and mechanism of methanol dehydrogenase. Biochimica et Biophysica Acta, 1647, 18–23. https://doi.org/10.1016/s1570-9639(03) 00042-6.
- Armstrong, J. D. (1964). The molar extinction coefficient of 2,6-dichlorophenol indophenol. *Biochimica et Biophysica Acta*, 86, 194–197. https://doi.org/10.1016/0304-4165(64) 90180-1.
- Barr, I., & Guo, F. (2015). Pyridine hemochromagen assay for determining the concentration of heme in purified protein solutions. *Bio-Protocol*, 5, e1594. https://doi.org/10.21769/ BioProtoc.1594.
- Chistoserdova, L. (2011). Modularity of methylotrophy, revisited. *Environmental Microbiology*, 13, 2603–2622. https://doi.org/10.1111/j.1462-2920.2011.02464.x.
- Chistoserdova, L. (2019). New pieces to the lanthanide puzzle. *Molecular Microbiology*, 111, 1127–1131. https://doi.org/10.1111/mmi.14210.
- Chistoserdova, L., & Kalyuzhnaya, M. G. (2018). Current trends in methylotrophy. *Trends in Microbiology*, 26, 703–714. https://doi.org/10.1016/j.tim.2018.01.011.
- Chistoserdova, L., Kalyuzhnaya, M. G., & Lidstrom, M. E. (2009). The expanding world of methylotrophic metabolism. *Annual Review of Microbiology*, 63, 477–499. https://doi.org/ 10.1146/annurev.micro.091208.073600.
- Choi, J. M., Cao, T.-P., Kim, S. W., Lee, K. H., & Lee, S. H. (2017). MxaJ structure reveals a periplasmic binding protein-like architecture with unique secondary structural elements. *Proteins*, 85, 1379–1386. https://doi.org/10.1002/prot.25283.
- Chu, F., Beck, D. A. C., & Lidstrom, M. E. (2016). MxaY regulates the lanthanide-mediated methanol dehydrogenase switch in Methylomicrobium buryatense. *PeerJ*, 4, e2435. https://doi.org/10.7717/peerj.2435.
- Clark, W. M. (1960). Oxidation-reduction potentials of organic systems. Baltimore: The Williams and Wilkins Company.
- Cook, E. C., Featherston, E. R., Showalter, S. A., & Cotruvo, J. A., Jr. (2019). Structural basis for rare earth element recognition by *Methylobacterium extorquens* lanmodulin. *Biochemistry*, 58, 120–125. https://doi.org/10.1021/acs.biochem.8b01019.
- Cotruvo, J. A., Jr. (2019). The chemistry of lanthanides in biology: Recent discoveries, emerging principles, and technological applications. *ACS Central Science*, *5*, 1496–1506. https://doi.org/10.1021/acscentsci.9b00642.
- Cotruvo, J. A., Jr., Featherston, E. R., Mattocks, J. A., Ho, J. V., & Laremore, T. N. (2018). Lanmodulin: A highly selective lanthanide-binding protein from a lanthanide-utilizing bacterium. *Journal of the American Chemical Society*, 140, 15056–15061. https://doi.org/10.1021/jacs.8b09842.
- Cox, J. M., Day, D. J., & Anthony, C. (1992). The interaction of methanol dehydrogenase and its electron acceptor, cytochrome ϵ_L in methylotrophic bacteria. *Biochimica et Biophysica Acta*, 1119, 97–106. https://doi.org/10.1016/0167-4838(92)90240-e.
- Day, D. J., & Anthony, C. (1990). Methanol dehydrogenase from *Methylobacterium extorquens* AM1. *Methods in Enzymology*, 188, 210–216. https://doi.org/10.1016/0076-6879(90) 88035-9.
- Deblonde, G. J.-P., Mattocks, J. A., Park, D. M., Reed, D. W., Cotruvo, J. A., Jr., & Jiao, Y. (2020). Selective and efficient biomacromolecular extraction of rare-earth elements using lanmodulin. *Inorganic Chemistry*, 59, 11855–11867. https://doi.org/10.1021/acs.inorgchem.0c01303.
- Dekker, R. H., Duine, J. A., Frank, J., Verweil, P. E. J., & Westerling, J. (1982). Covalent addition of H₂O, enzyme substrates and activators to pyrrolo-quinoline quinone, the

- coenzyme of quinoproteins. *European Journal of Biochemistry*, 125, 69–73. https://doi.org/10.1111/j.1432-1033.1982.tb06652.x.
- Delaney, N. F., Kaczmarek, M. E., Ward, L. M., Swanson, P. K., Lee, M.-C., & Marx, C. J. (2013). Development of an optimized medium, strain and high-throughput culturing methods for *Methylobacterium extorquens*. *PLoS One*, 8, e62957. https://doi.org/10. 1371/journal.pone.0062957.
- Drake, S. K., Lee, K. L., & Falke, J. J. (1996). Tuning the equilibrium ion affinity and selectivity of the EF-hand calcium binding motif: Substitutions at the gateway position. *Biochemistry*, 35, 6697–6705. https://doi.org/10.1021/bi952430l.
- Duine, J. A. (1999). The PQQ story. Journal of Bioscience and Bioengineering, 88, 231–236. https://doi.org/10.1016/S1389-1723(00)80002-X.
- Edington, S. C., Gonzalez, A., Middendorf, T. R., Halling, D. B., Aldrich, R. W., & Baiz, C. R. (2018). Coordination to lanthanide ions distorts binding site conformation in calmodulin. *Proceedings. National Academy of Sciences. United States of America*, 115, E3126–E3134. https://doi.org/10.1073/pnas.1722042115.
- Efimov, I., Parkin, G., Millett, E. S., Glenday, J., Chan, C. K., Weedon, H., et al. (2014). A simple method for the determination of reduction potentials in heme proteins. *FEBS Letters*, *588*, 701–704. https://doi.org/10.1016/j.febslet.2013.12.030.
- Englard, S., & Seifter, S. (1990). Precipitation techniques. *Methods in Enzymology*, 182, 287–300. https://doi.org/10.1016/0076-6879(90)82024-v.
- Farhan Ul Haque, M., Kalidass, B., Bandow, N., Turpin, E. A., DiSpirito, A. A., & Semrau, J. D. (2015). Cerium regulates expression of alternative methanol dehydrogenases in Methylosinus trichosporium OB3b. Applied and Environmental Microbiology, 81, 7546–7552. https://doi.org/10.1128/AEM.02542-15.
- Featherston, E. R., & Cotruvo, J. A., Jr. (2021). The biochemistry of lanthanide acquisition, trafficking, and utilization. *Biochimica et Biophysica Acta, Molecular Cell Research*, 1868, 118864. https://doi.org/10.1016/j.bbamcr.2020.118864.
- Featherston, E. R., Rose, H. R., McBride, M. J., Taylor, E. M., Boal, A. K., & Cotruvo, J. A., Jr. (2019). Biochemical and structural characterization of XoxG and XoxJ and their roles in lanthanide-dependent methanol dehydrogenase activity. *Chembiochem*, 20, 2360–2372. https://doi.org/10.1002/cbic.201900184.
- Fitriyanto, N. A., Fushimi, M., Matsunaga, M., Pertiwiningrum, A., Iwama, T., & Kawai, K. (2011). Molecular structure and gene analysis of Ce³⁺-induced methanol dehydrogenase of *Bradyrhizobium* sp. MAFF211645. *Journal of Bioscience and Bioengineering*, 111, 613–617. https://doi.org/10.1016/j.jbiosc.2011.01.015.
- Gasteiger, E., Hoogland, C., Gattiker, A., Duvaud, S., Wilkins, M. R., Appel, R. D., et al. (2005). Protein identification and analysis tools on the ExPASy server. In J. M. Walker (Ed.), *The proteomics protocols handbook* (pp. 571–607). Totowa, NJ: Humana Press. https://doi.org/10.1385/1-59259-890-0:571.
- Gifford, J. L., Walsh, M. P., & Vogel, H. J. (2007). Structures and metal-ion-binding properties of the Ca²⁺-binding helix-loop-helix EF-hand motifs. *The Biochemical Journal*, 405, 199–221. https://doi.org/10.1042/BJ20070255.
- Good, N. M., Moore, R. S., Suriano, C. J., & Martinez-Gomez, N. C. (2019). Contrasting in vitro and in vivo methanol oxidation activities of lanthanide-dependent alcohol dehydrogenases XoxF1 and ExaF from *Methylobacterium extorquens* AM1. *Scientific Reports*, 9, 4248. https://doi.org/10.1038/s41598-019-41043-1.
- Good, N. M., Vu, H. N., Suriano, C. J., Subuyuj, G. A., Skovran, E., & Martinez-Gomez, N. C. (2016). Pyrroloquinoline quinone ethanol dehydrogenase in *Methylobacterium extorquens* AM1 extends lanthanide-dependent metabolism to multicarbon substrates. *Journal of Bacteriology*, 198, 3109–3118. https://doi.org/10.1128/JB.00478-16.
- Gu, W., Haque, M. F. U., Dispirito, A. A., & Semrau, J. D. (2016). Uptake and effect of rare earth elements on gene expression in *Methylosinus trichosporium* OB3b. *FEMS Microbiology Letters*, 363, fnw129. https://doi.org/10.1093/femsle/fnw129.

- Gu, W., & Semrau, J. D. (2017). Copper and cerium-regulated gene expression in Methylosinus trichosporium OB3b. *Applied Microbiology and Biotechnology*, 101, 8499–8516. https://doi.org/10.1007/s00253-017-8572-2.
- Hibi, Y., Asai, K., Arafuka, H., Hamajima, M., Iwama, T., & Kawai, K. (2011). Molecular structure of La³⁺-induced methanol dehydrogenase-like protein in *Methylobacterium radiotolerans*. *Journal of Bioscience and Bioengineering*, 111, 547–549. https://doi.org/10.1016/j.jbiosc.2010.12.017.
- Ho, J. V., & Cotruvo, J. A., Jr. (2019). A periplasmic binding protein for pyrroloquinoline quinone. *Biochemistry*, 58, 2665–2669. https://doi.org/10.1021/acs.biochem.9b00358.
- Huang, J., Yu, Z., & Chistoserdova, L. (2018). Lanthanide-dependent methanol dehydrogenases of XoxF4 and XoxF5 clades are differentially distributed among methylotrophic bacteria and they reveal different biochemical properties. Frontiers in Microbiology, 9, 1366. https://doi.org/10.3389/fmicb.2018.01366.
- Huang, J., Yu, Z., Groom, J., Cheng, J. F., Tarver, A., Yoshikuni, Y., et al. (2019). Rare earth element alcohol dehydrogenases widely occur among globally distributed, numerically abundant and environmentally important microbes. *The ISME Journal*, 13, 2005–2017. https://doi.org/10.1038/s41396-019-0414-z.
- Indyk, L., & Fisher, H. F. (1998). Theoretical aspects of isothermal titration calorimetry. Methods in Enzymology, 295, 350–364. https://doi.org/10.1016/s0076-6879(98)95048-0.
- Kalimuthu, P., Daumann, L. J., Pol, A., Op den Camp, H. J. M., & Bernhardt, P. V. (2019). Electrocatalysis of a europium-dependent bacterial methanol dehydrogenase with its physiological electron acceptor cytochrome c_{GJ} . Chemistry—A European Journal, 25, 8760–8768. https://doi.org/10.1002/chem.201900525.
- Keltjens, J. T., Pol, A., Reimann, J., & Op den Camp, H. J. M. (2014). PQQ-dependent methanol dehydrogenases: Rare-earth elements make a difference. *Applied Microbiology* and Biotechnology, 98, 6163–6183. https://doi.org/10.1007/s00253-014-5766-8.
- Koehn, E. M., Latham, J. A., Armand, T., Evans, R. L., Tu, X., Wilmot, C. M., et al. (2019). Discovery of hydroxylase activity for PqqB provides a missing link in the pyrroloquinoline quinone biosynthetic pathway. *Journal of the American Chemical Society*, 141, 4398–4405. https://doi.org/10.1021/jacs.8b13453.
- Krause, S. M. B., Johnson, T., Samadhi Karunaratne, Y., Fu, Y., Beck, D. A. C., Chistoserdova, L., et al. (2017). Lanthanide-dependent cross-feeding of methanederived carbon is linked by microbial community interactions. *Proceedings of the National Academy of Sciences of the United States of America*, 114, 358–363. https://doi. org/10.1073/pnas.1619871114.
- Londer, Y. Y. (2011). Expression of recombinant cytochromes c in E. coli. In J. T. C. Evans, & M.-Q. Xu (Eds.), Heterologous gene expression in E. coli: Methods and protocols (pp. 123–150). Totowa, NJ: Humana Press. https://doi.org/10.1007/978-1-61737-967-3 8.
- Lumpe, H., & Daumann, L. J. (2019). Studies of redox cofactor pyrroloquinoline quinone and its interaction with lanthanides(III) and calcium(II). *Inorganic Chemistry*, 58, 8432–8441. https://doi.org/10.1021/acs.inorgchem.9b00568.
- Lumpe, H., Pol, A., Op den Camp, H. J. M., & Daumann, L. J. (2018). Impact of the lanthanide contraction on the activity of a lanthanide-dependent methanol dehydrogenase—A kinetic and DFT study. *Dalton Transactions*, 47, 10463–10472. https://doi.org/10.1039/c8dt01238e.
- Lyle, S. J., & Rahman, M. M. (1963). Complexometric titration of yttrium and the lanthanons—I: A comparison of direct methods. *Talanta*, 10, 1177–1182. https://doi. org/10.1016/0039-9140(63)80170-8.
- Magnusson, O. T., RoseFigura, J. M., Toyama, H., Schwarzenbacher, R., & Klinman, J. P. (2007). Pyrroloquinoline quinone biogenesis: Characterization of PqqC and its H84N and H84A active site variants. *Biochemistry*, 46, 7174–7186. https://doi.org/10.1021/bi700162n.

- Massey, V. (1991). A simple method for determination of redox potentials. In B. Curtis, S. Roncho, & G. Zanetti (Eds.), *Flavins and flavoproteins 1990* (pp. 59–66). Berlin: Walter de Gruyter & Co.
- Masuda, S., Suzuki, Y., Fujitani, Y., Mitsui, R., Nakagawa, T., Shintani, M., et al. (2018). Lanthanide-dependent regulation of methylotrophy in *Methylobacterium aquaticum* strain 22A. mSphere, 3, e00462-00417. https://doi.org/10.1128/mSphere.00462-17.
- Mattocks, J. A., Ho, J. V., & Cotruvo, J. A., Jr. (2019). A selective, protein-based fluorescent sensor with picomolar affinity for rare earth elements. *Journal of the American Chemical Society*, 141, 2857–2861. https://doi.org/10.1021/jacs.8b12155.
- Munshi, K. N., & Dey, A. K. (1968). Absorptiometric study of the chelates formed between the lanthanoids and xylenol orange. *Microchimica Acta*, *56*, 1059–1065. https://doi.org/10.1007/BF01221178.
- Nakagawa, T., Mitsui, R., Tani, A., Sasa, K., Tashiro, S., Iwama, T., et al. (2012). A catalytic role of XoxF1 as La³⁺-dependent methanol dehydrogenase in *Methylobacterium extorquens* strain AM1. *PLoS One*, 7, e50480. https://doi.org/10.1371/journal.pone.0050480.
- Ochsner, A. M., Hemmerle, L., Vonderach, T., Nüssli, R., Bortfeld-Miller, M., Hattendorf, B., et al. (2019). Use of rare earth elements in the phyllosphere colonizer *Methylobacterium extorquens* PA1. *Molecular Microbiology*, 111, 1152–1166. https://doi.org/10.1111/mmi.14208.
- O'Keeffe, D. T., & Anthony, C. (1980). The two cytochromes c in the facultative methylotroph *Pseudomonas* AM1. *The Biochemical Journal*, 192, 411–419. https://doi.org/10.1042/bj1920411.
- Picone, N., & Op den Camp, H. J. M. (2019). Role of rare earth elements in methanol oxidation. Current Opinion in Chemical Biology, 49, 39–44. https://doi.org/10.1016/j.cbpa. 2018.09.019.
- Pierce, M. M., Raman, C. S., & Nall, B. T. (1999). Isothermal titration calorimetry of protein–protein interactions. *Methods*, 19, 213–221. https://doi.org/10.1006/meth. 1999.0852.
- Pol, A., Barends, T. R. M., Dietl, A., Khadem, A. F., Eygensteyn, J., Jetten, M. S. M., et al. (2014). Rare earth metals are essential for methanotrophic life in volcanic mudpots. *Environmental Microbiology*, 16, 255–264. https://doi.org/10.1111/1462-2920.12249.
- Quinn, C. F., Carpenter, M. C., Croteau, M. L., & Wilcox, D. E. (2016). Isothermal titration calorimetry measurements of metal ions binding to proteins. *Methods in Enzymology*, 567, 3–21. https://doi.org/10.1016/bs.mie.2015.08.021.
- Roszczenko-Jasińska, P., Vu, H. N., Subuyuj, G. A., Crisostomo, R. V., Cai, J., Lien, N. F., et al. (2020). Gene products and processes contributing to lanthanide homeostasis and methanol metabolism in *Methylorubrum extorquens* AM1. *Scientific Reports*, 10, 12663. https://doi.org/10.1038/s41598-020-69401-4.
- Scheepers, G. H., Lycklama a Nijeholt, J. A., & Poolman, B. (2016). An updated structural classification of substrate-binding proteins. *FEBS Letters*, *590*, 4393–4401. https://doi.org/10.1002/1873-3468.12445.
- Shelton, A. N., Seth, E. C., Mok, K. C., Han, A. W., Jackson, S. N., Haft, D. R., et al. (2019). Uneven distribution of cobamide biosynthesis and dependence in bacteria predicted by comparative genomics. *The ISME Journal*, 13, 789–804. https://doi.org/ 10.1038/s41396-018-0304-9.
- Skovran, E., Raghuraman, C., & Martinez-Gomez, N. C. (2019). Lanthanides in methylotrophy. Current Issues in Molecular Biology, 33, 101–116. https://doi.org/10. 21775/cimb.033.101.
- Taubert, M., Grob, C., Howat, A. M., Burns, O. J., Dixon, J. L., Chen, Y., et al. (2015). XoxF encoding an alternative methanol dehydrogenase is widespread in coastal marine environments. *Environmental Microbiology*, 17, 3937–3948. https://doi.org/10.1111/ 1462-2920.12896.

- Tonosaki, K., & Otomo, M. (1962). Spectrophotometric determination of cerium(III) and some rare earths with xylenol orange. *Bulletin of the Chemical Society of Japan*, 35, 1683–1686. https://doi.org/10.1246/bcsj.35.1683.
- van Kleef, M. A., & Duine, J. A. (1989). Factors relevant in bacterial pyrroloquinoline quinone production. *Applied and Environmental Microbiology*, *55*, 1209–1213. https://doi.org/10.1128/aem.55.5.1209-1213.1989.
- Van Spanning, R. J., Wansell, C. W., De Boer, T., Hazelaar, M. J., Anazawa, H., Harms, N., et al. (1991). Isolation and characterization of the moxJ, moxG, moxI, and moxR genes of Paracoccus denitrificans: Inactivation of moxJ, moxG, and moxR and the resultant effect on methylotrophic growth. *Journal of Bacteriology*, 173, 6948–6961. https://doi.org/10.1128/jb.173.21.6948-6961.1991.
- Versantvoort, W., Pol, A., Daumann, L. J., Larrabee, J. A., Strayer, A. H., Jetten, M. S. M., et al. (2019). Characterization of a novel cytochrome $\epsilon_{\rm GJ}$ as the electron acceptor of XoxF-MDH in the thermoacidophilic methanotroph *Methylacidiphilum fumariolicum* SolV. *Biochimica et Biophysica Acta, Proteins and Proteomics*, 1867, 595–603. https://doi.org/10.1016/j.bbapap.2019.04.001.
- Vu, H. N., Subuyuj, G. A., Vijayakumar, S., Good, N. M., Martinez-Gomez, N. C., & Skovran, E. (2016). Lanthanide-dependent regulation of methanol oxidation systems in *Methylobacterium extorquens* AM1 and their contribution to methanol growth. *Journal of Bacteriology*, 198, 1250–1259. https://doi.org/10.1128/JB.00937-15.
- Wang, L., Hibino, A., Suganuma, S., Ebihara, A., Iwamoto, S., Mitsui, R., et al. (2020). Preference for particular lanthanide species and thermal stability of XoxFs in Methylorubrum extorquens strain AM1. Enzyme and Microbial Technology, 136, 109518. https://doi.org/10.1016/j.enzmictec.2020.109518.
- Wegner, C.-E., Gorniak, L., Riedel, S., Westermann, M., & Küsel, K. (2019). Lanthanide-dependent methylotrophs of the family Beijerinckiaceae: Physiological and genomic insights. *Applied and Environmental Microbiology*, 86(1), e01830-01819. https://doi.org/10.1128/AEM.01830-19.
- Wehrmann, M., Berthelot, C., Billard, P., & Klebensberger, J. (2018). The PedS2/PedR2 two-component system is crucial for the rare earth element switch in *Pseudomonas putida* KT2440. *mSphere*, *3*, e00376-00318. https://doi.org/10.1128/mSphere.00376-18.
- Wehrmann, M., Billard, P., Martin-Meriadec, A., Zegeye, A., & Klebensberger, J. (2017). Functional role of lanthanides in enzymatic activity and transcriptional regulation of pyrroloquinoline quinone-dependent alcohol dehydrogenases in *Pseudomonas putida* KT2440. mBio, 8, e00570-00517. https://doi.org/10.1128/mBio.00570-17.
- Williams, P., Coates, L., Mohammed, F., Gill, R., Erskine, P., Bourgeois, D., et al. (2006). The 1.6 Å x-ray structure of the unusual *c*-type cytochrome, cytochrome *c*_L, from the methylotrophic bacterium *Methylobacterium extorquens*. *Journal of Molecular Biology*, *357*, 151–162. https://doi.org/10.1016/j.jmb.2005.12.055.
- Zheng, Y., Huang, J., Zhao, F., & Chistoserdova, L. (2018). Physiological effect of XoxG(4) on lanthanide-dependent methanotrophy. *mBio*, 9, e02430-02417. https://doi.org/10.1128/mBio.02430-17.
- Zhu, W., & Klinman, J. P. (2020). Biogenesis of the peptide-derived redox cofactor pyrroloquinoline quinone. Current Opinion in Chemical Biology, 59, 93–103. https:// doi.org/10.1016/j.cbpa.2020.05.001.